Rivelatori per neutrini (extra)galattici di altissime energie

Reazioni tipiche:

ν_μ + N → μ^- + adroni
ν_e + N → e^- + adroni

Piccolissime sezioni d'urto → necessari enormi volumi di materiale per avere un ragionevole numero di eventi

Nei primi rivelatori sviluppati/in costruzione: solo misura del μ nella prima delle reazioni. Rivelazione dell'elettrone possibile, ma relativa efficienza bassa.

Importante uno studio dettagliato delle caratteristiche di propagazione del μ nella roccia/acqua/ghiaccio→

Perdite d'energia dei μ underground

Profondita' atmosferica: X~ 1000 $g x cm^{-2}$
Sotto 1 km di roccia: X → $2.65 x 10^5$ $g x cm^{-2}$
Spesso espressa in km di acqua equivalente (1 km a.e.=10^5 $g x cm^{-2}$)
A densita' cosi' elevate il μ subisce, oltre alla perdita d'energia per ionizzazione (all'incirca indipendente dall'energia e pari a circa 2 MeV g^{-1} cm^2), anche:
-bremsstrahlung
-produzione di coppie elettrone-positrone
-fotoproduzione
Questi sono proporzionali all'energia →

$$\frac{dE}{dx} = -a - bE_\mu$$

$$b = b_{br} + b_{pair} + b_{ph}; \qquad \text{Roccia}: b \cong 4 \times 10^{-6} \quad \left(g^{-1}\, cm^2\right)$$

Energia critica ⇒ perdita d'energia per ionizzazione = perdita d'energia per processi radiativi:

$$a = bE_\mu \Rightarrow E_{cr} = \frac{a}{b} \equiv \varepsilon \cong 500\, GeV$$

Perdita d'energia dominata da effetti radiativi per E_μ molto maggiore di ε

Perdita d'energia dominata da ionizzazione per E_μ molto minore di ε

Contributi relativi alla perdita d'energia per radiazione dei μ undeground

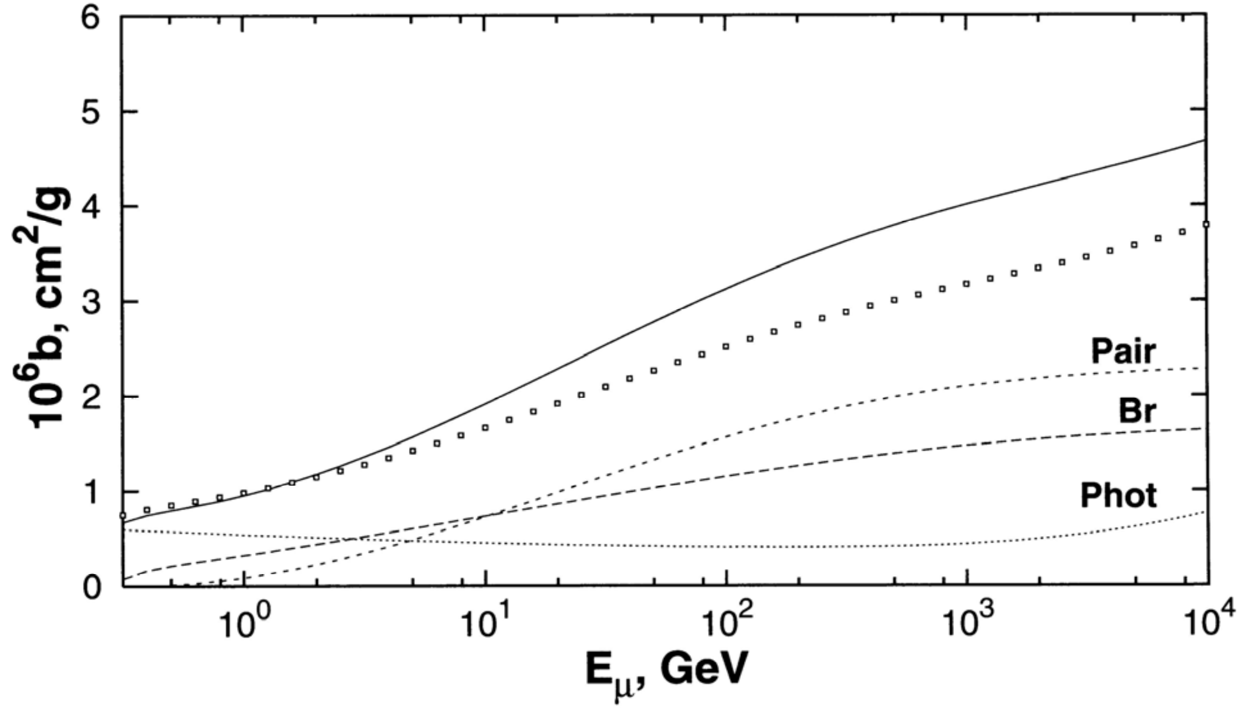

Fig. 7.4. Relative energy loss on radiation in standard rock. Solid line shows the sum of the three processes. Circles show the b value for clean ice.

Perdite d'energia dei μ underground

$$\frac{dE}{dx} = -a - bE_{\mu}$$

$$E_{cr} = \frac{a}{b} \equiv \varepsilon \cong 500\ GeV$$

Energia di un μ avente energia iniziale E_{μ}^{0} dopo un percorso X nella roccia :

$$E_{\mu}(X) = \left(E_{\mu}^{0} + \varepsilon\right) \times e^{-bX} - \varepsilon$$

Minima energia che un μ deve avere per penetrare ad una profondita' X :

$$\left(E_{\mu}^{\min} + \varepsilon\right) \times e^{-bX} - \varepsilon = 0 \Rightarrow E_{\mu}^{\min} = \varepsilon\left[e^{bX} - 1\right]$$

Per piccole profondita' $(bX << 1)$, sviluppando l'esponenziale $\Rightarrow E_{\mu}^{\min} = \varepsilon[1 + bX - 1] = aX$

Cioe' la perdita d'energia avviene sopratutto per ionizzazione $\Rightarrow$ spettro osservato dei μ riflette quello in superficie, appiattito per $E_{\mu} \le aX$.

Per grandi X ed $E_{\mu} \le \varepsilon \Rightarrow E_{\mu} \approx (2\varepsilon) \times e^{-bX} - \varepsilon = \varepsilon\left(e^{-bX} - 1\right) =$ cost.

Per grandi X ed $E_{\mu} \ge \varepsilon \Rightarrow E_{\mu} \approx \left(E_{\mu}^{0} + \varepsilon\right) \times e^{-bX} - \varepsilon \Rightarrow$ spettro cade piu' velocemente di quello iniziale

Flusso di μ underground

Relazione profondita'-flusso

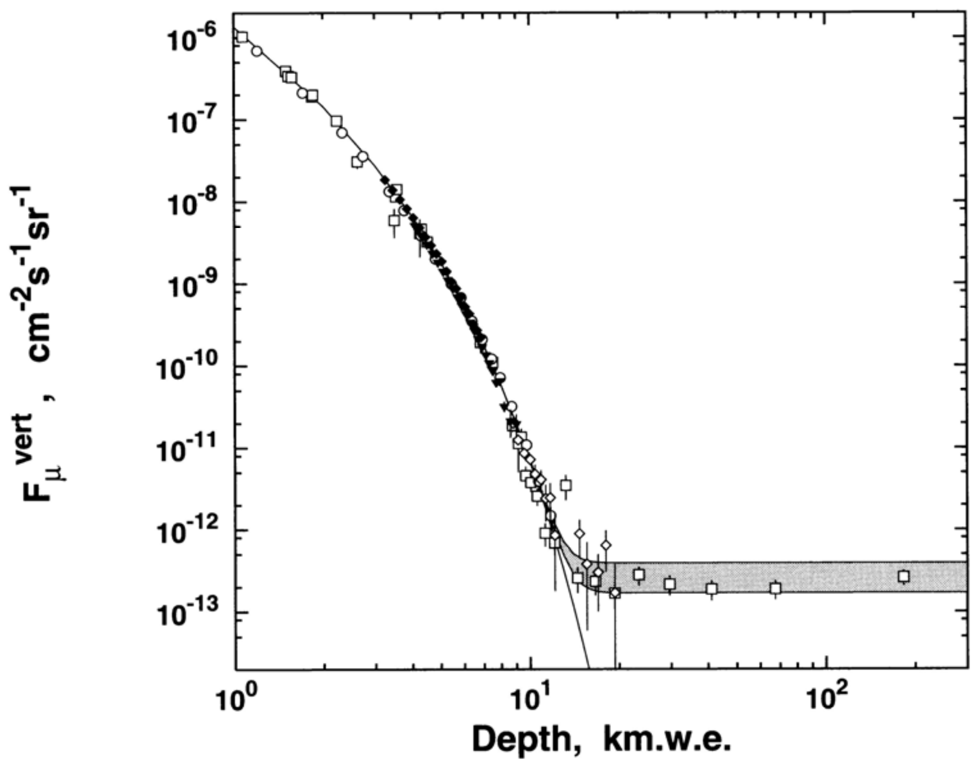

Fig. 7.1. Depth–intensity relation – the integral muon flux measured at different depths and angles and converted to vertical muon flux is compared to predictions. See text for the references to different data sets.

Perdite d'energia dei μ underground

Range di un μ :

$$R(E_\mu) = \frac{1}{b}\ln\left(\frac{E_\mu}{\varepsilon} + 1\right)$$

Ipotesi che la perdita d'energia sia continua (ionizzazione). Cioe' fino a circa 100 GeV. Non vera per i processi radiativi (dominati da pochi eventi con grosse perdite d'energia.

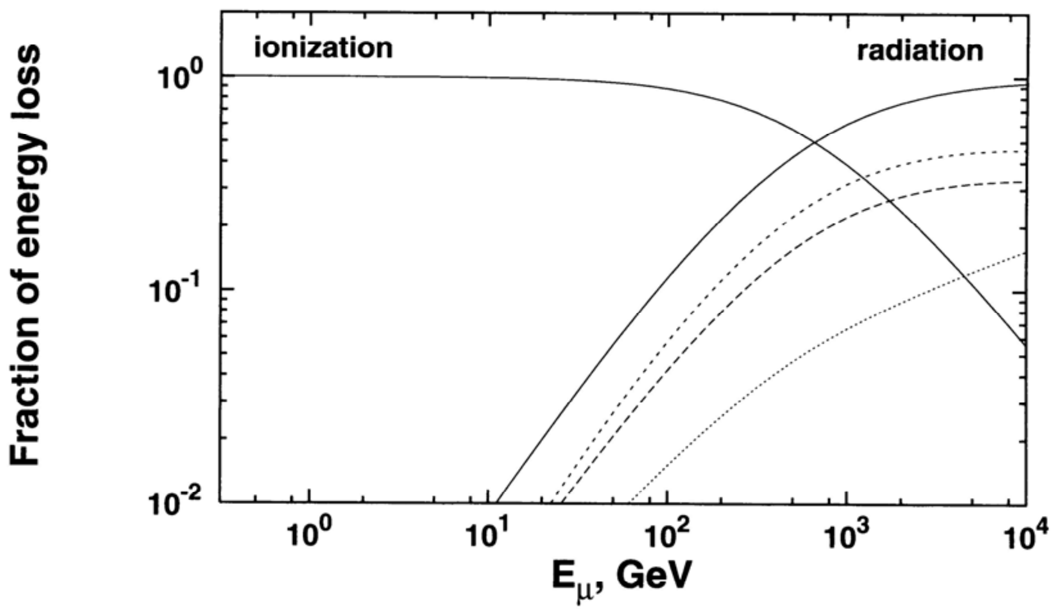

Fig. 7.2. Relative importance of different radiation processes as a function of the muon energy normalized to the total energy loss per g/cm^2. The long-dashed curve is for bremsstrahlung, the short-dashed curve for direct pair-production, and the dotted curve for photoproduction.

Probabilita' di penetrazione dei μ underground

Mesoni μ che non subiscono processi radiativi possono propagarsi molto oltre la profondita' X.
Confronto di $\langle R_\mu \rangle$ con R. Rapporto $\langle R_\mu \rangle / R$ dipende dall'energia.
Nella pratica si ricorre a simulazioni MC piuttosto che al calcolo analitico.

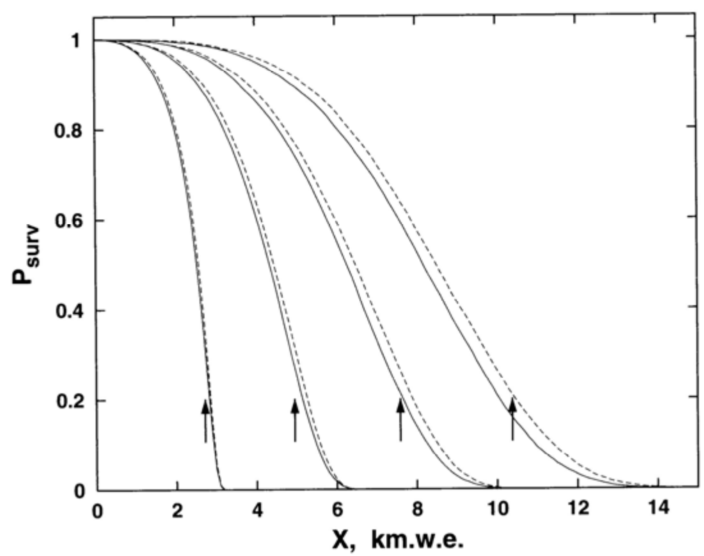

Fig. 7.3. Survival probability of muons with energy of 1., 3.16, 10., and 31.6 TeV in standard rock. The two curves for each energy indicate the uncertainties in the bremsstrahlung cross-section as stated in below. The arrows show the average depth for muon survival calculated from (7.4).

Neutrini cosmici

Neutrini osservati nella radiazione cosmica:

a) dal Sole
b) dalla SN1987A
   Energie di pochi MeV
c) dai raggi cosmici (decadimenti dei π)
Energie fino a qualche decina di GeV

Osservazione di neutrini di alte energie da sorgenti Galattiche ?

Vantaggi dei neutrini:
a) poco assorbiti dal materiale della sorgente in cui sono prodotti → informazioni sul nucleo della sorgente
b) poco assorbiti dal mezzo Galattico/Intergalattico
c) non deflessi da campi magnetici

Fotoni fortemente assorbiti per energie superiori a 10^{13} eV (interazione con il CMB)

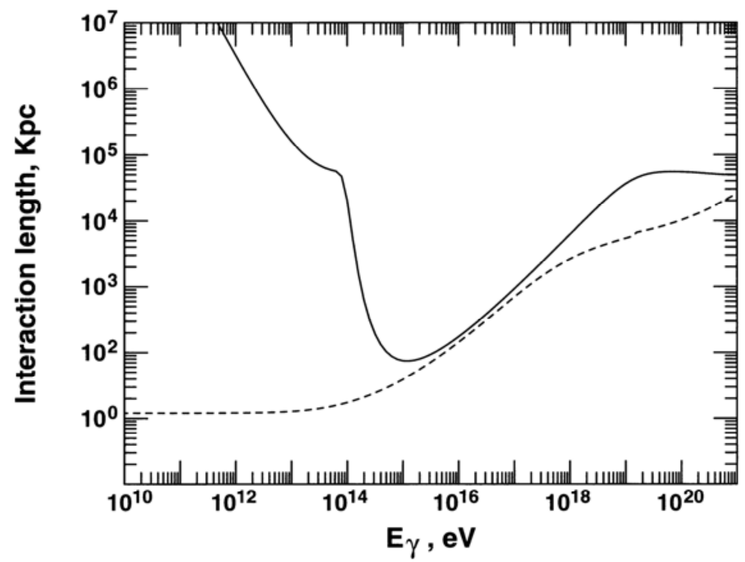

Fig. 10.1. Interaction length for γ-ray (solid) and electron (dashed line) interactions on the universal photon backgrounds. Only the major process of production of electron–positron pairs is plotted for gamma-rays. The electron interaction length is shown for inverse Compton effect.

Neutrini cosmici

Inoltre i neutrini possono aiutarci a discriminare tra modelli di produzione adronica/leptonica in SN, AGN, etc.

Svantaggi dei neutrini:
piccola sezione d'urto, anche ad alte energie (circa 10 ordini di grandezza inferiore a quella dei fotoni)

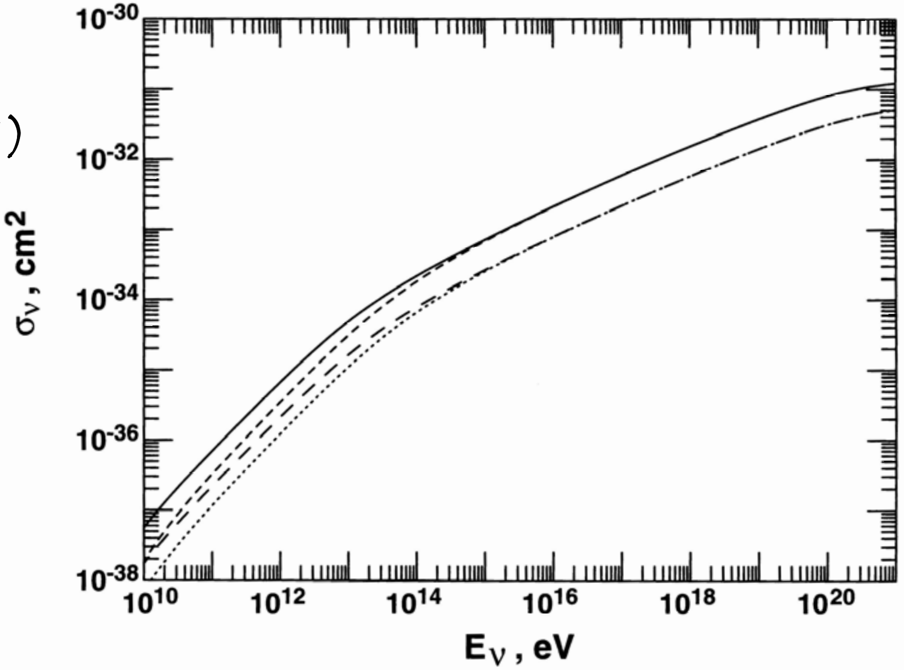

Fig. 10.2. Cross-sections for deep inelastic neutrino scattering. Neutrino CC cross-section is plotted with a solid line, the antineutrino with short dashes. The NC cross-section for neutrinos are plotted with long dashes, and for antineutrinos with a dotted line.

Neutrini cosmici

Neutrini prodotti in oggetti Galattici/Extragalattici:

$p + p \rightarrow p(n) + m\,\pi^0 + 2m\,\pi^{+/-}$

$\pi^{+/-} \rightarrow \mu^{+/-}\,\nu$

$\pi^0 \rightarrow \gamma\,\gamma$

Produzione di neutrini e fotoni in sistemi binari

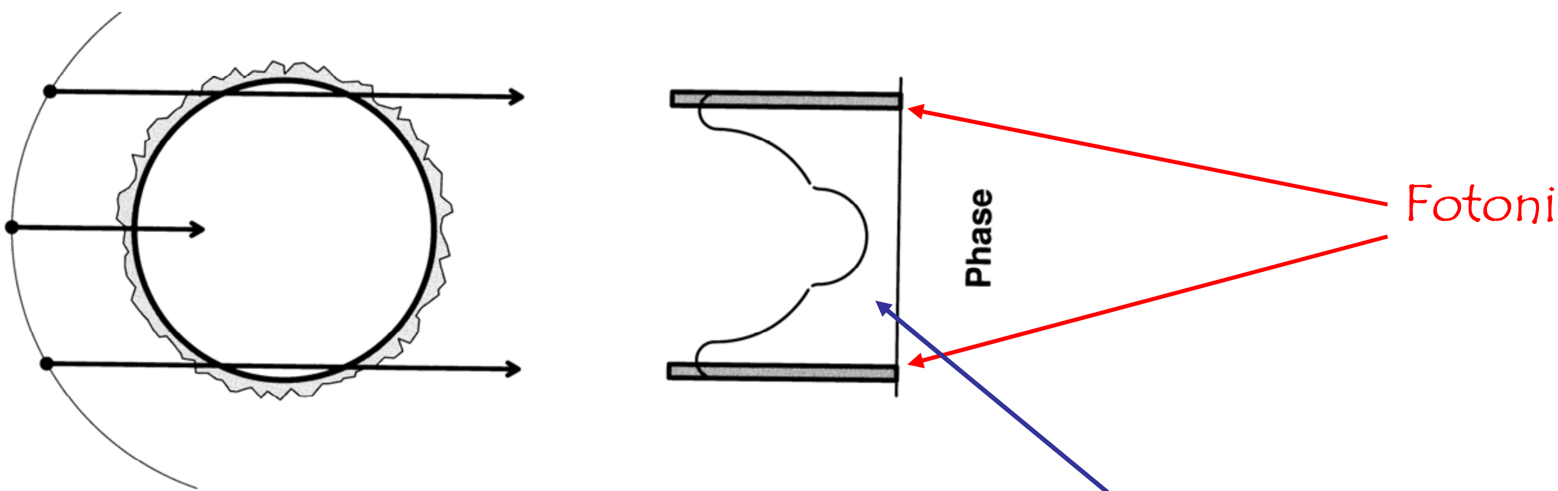

Fig. 10.3. The Vestrand–Eichler model of signal production in a binary system and the light curve for γ-ray (shaded) and neutrino fluxes.

Neutrini cosmici da AGN

Alla produzione di fotoni attraverso il meccanismo SSC (Synchrotron-Self-Compton) si somma la produzione attraverso il meccanismo adronico → fotoni di energie piu' elevate e neutrini

π carichi prodotti in reazioni di fotoproduzione:

$p + \gamma \rightarrow p(n) + m\ \pi^{+/-} + n\ \pi^{0}$

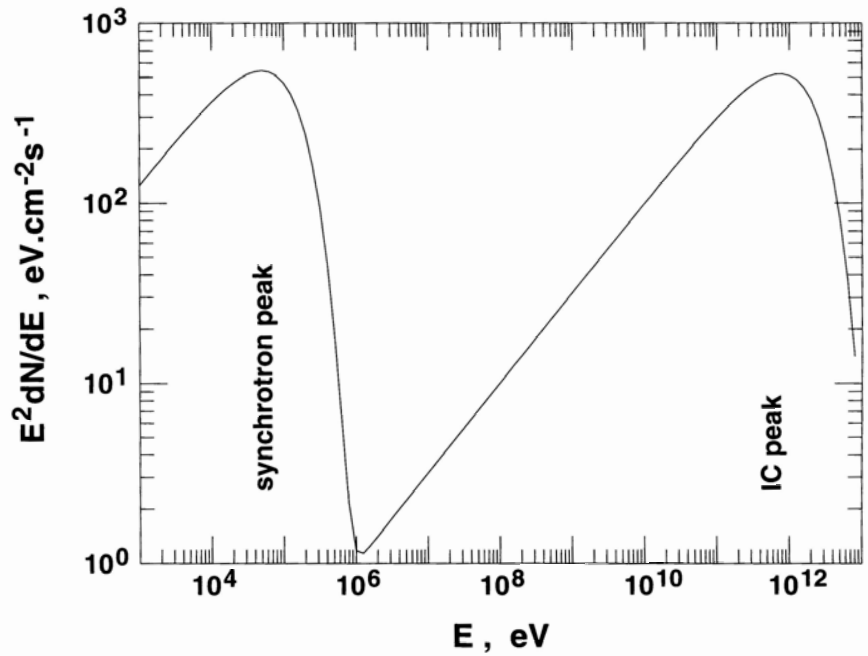

Fig. 10.9. Two-peaked photon spectrum generated by the Synchrotron Self Compton model of γ-ray production.

Neutrini cosmici da sorgenti note

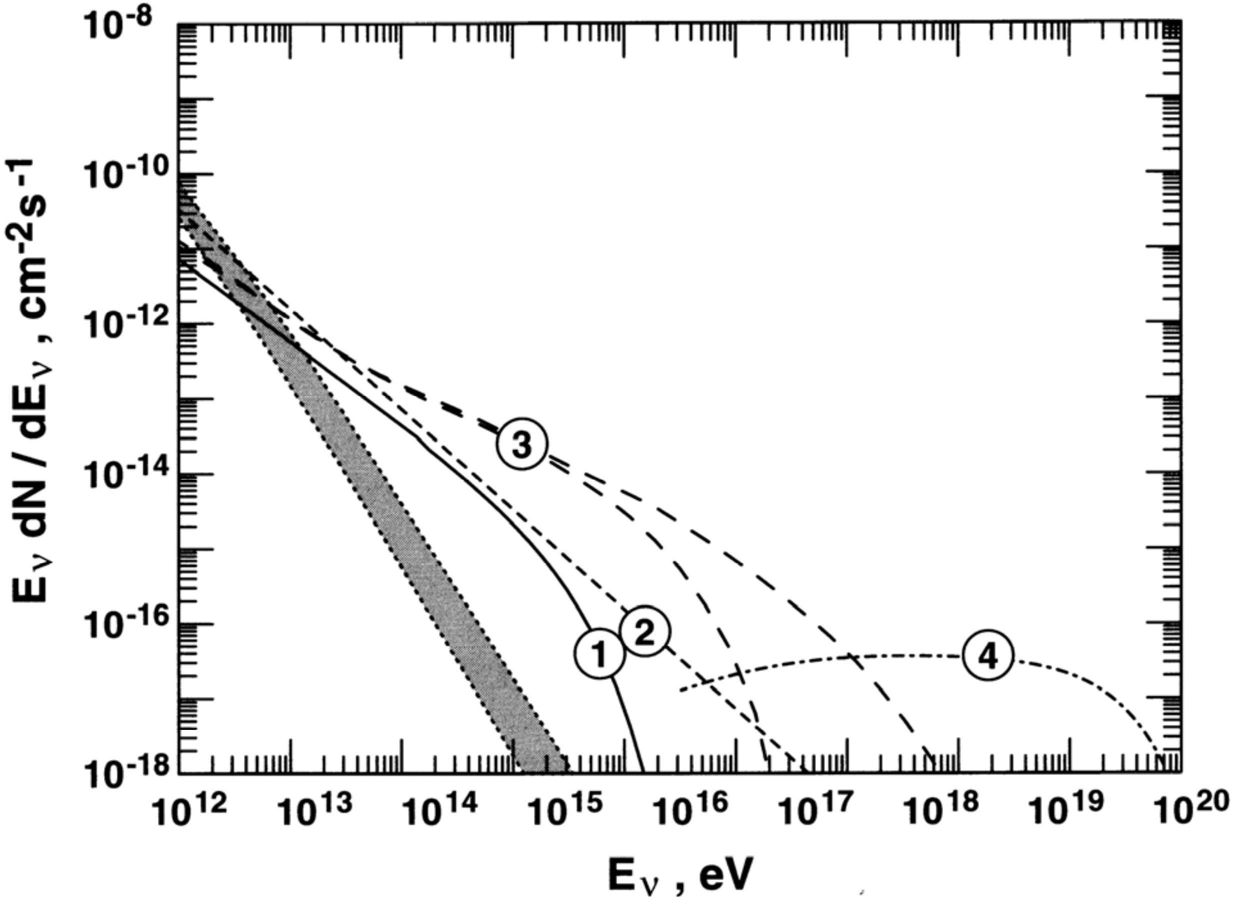

Fig. 10.12. Predictions of neutrino fluxes from different types of sources. (1) is the neutrino flux that would correspond to the gamma-rays of SNR IC443. (2) is the neutrino emission that would correspond to hadronic origin of the Mrk 501 gamma-ray outburst. (3) is the range of neutrino emission from the core of 3C273, and 4) is a prediction for the neutrino emission of 3C279. The shaded are shows the atmospheric neutrino flux within 1° – from high (horizontal) to vertical.

Neutrini cosmici diffusi

Fondo da neutrini prodotti in interazioni dei raggi cosmici nell'atmosfera: spettro molto piu' ripido (concentrato a basse energie)

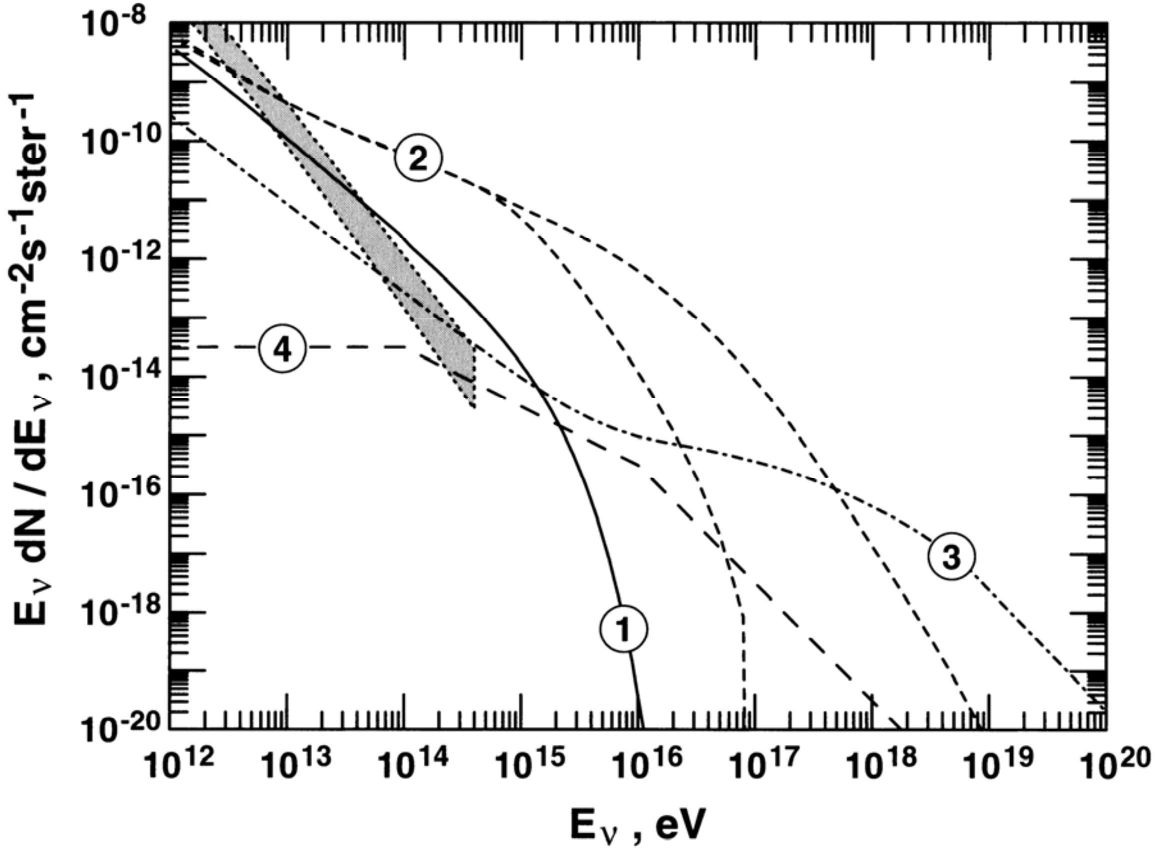

Fig. 10.13. Predictions for diffuse neutrino fluxes. The shaded area shows the horizontal (higher) and vertical fluxes of atmospheric neutrinos. Curve (1) is for the central region of the Galaxy, (2) corresponds to the curves (3) from Fig. 10.12, (3) is the prediction of Ref. [359] and (4) is the prediction of the GRB neutrinos of Ref. [358].

Rivelatori

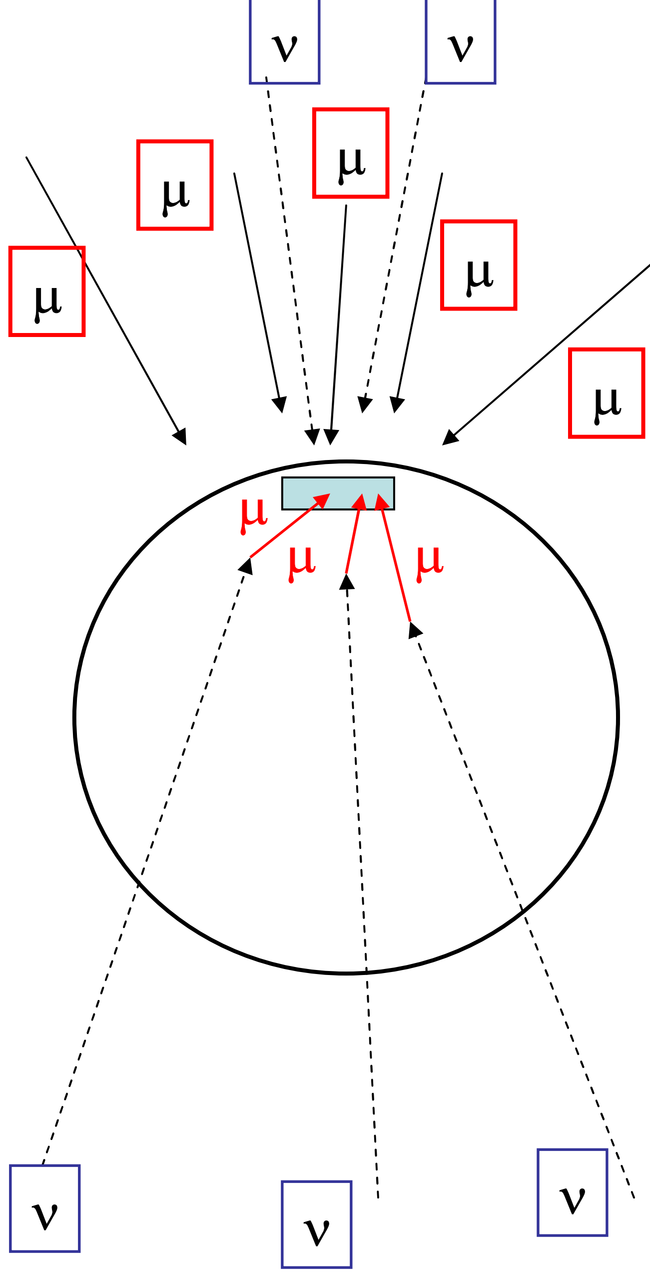

Rivelatori posti nell'emisfero Nord "guardano" verso il basso

Rivelatori posti nell'emisfero Sud "guardano" verso l'alto

Reazioni utilizzabili :

$$\nu_\mu + N \rightarrow \mu^- + adroni \quad (p, n, \pi^\pm, \pi^0, K^\pm, K^0 ....)$$

$$\bar{\nu}_\mu + N \rightarrow \mu^+ + adroni$$

Il mesone μ prodotto nell'interazione del <u>neutrino</u> ha circa meta' dell'energia di questo. Ad energie molto elevate viaggia nella medesima direzione del neutrino.

Rivelatori

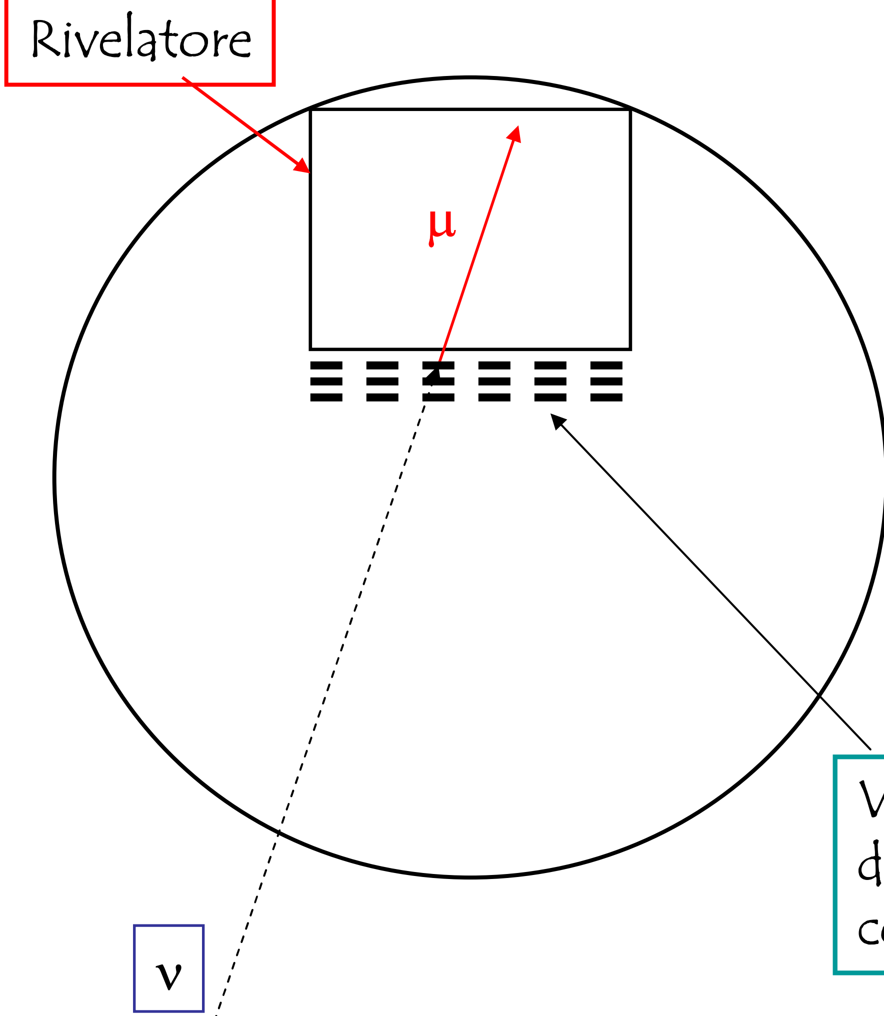

Reazioni utilizzabili :

$$\nu_\mu + N \rightarrow \mu^- + adroni \quad \left(p, n, \pi^\pm, \pi^0, K^\pm, K^0 \ldots\ldots\right)$$

$$\bar{\nu}_\mu + N \rightarrow \mu^+ + adroni$$

Direzione ed energia del mesone μ misurate attraverso la rivelazione della luce Cerenkov emessa in acqua

Volume utile molto maggiore del volume del rivelatore (utilizzo della roccia sottostante come "bersaglio")

Neutrinos weakly interacting in matter

Low cross-section

good :

Astronomic sources and universe transparent to neutrinos

Earth transparent up to 100 TeV

bad:

Need massive detector

Interaction length of neutrinos vs energy

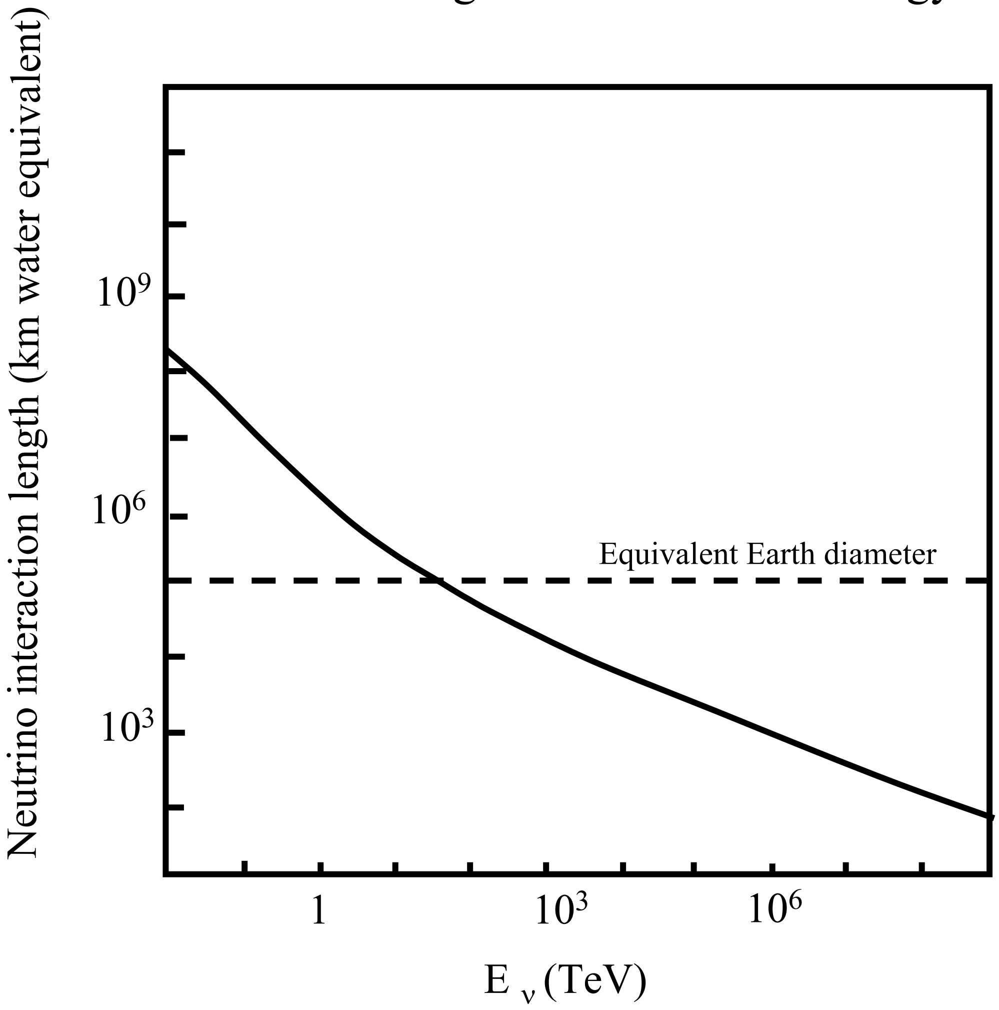

Neutrino Interactions in water/earth

3 flavours of neutrino, 2 types of interaction: 4 topologies of light production in water

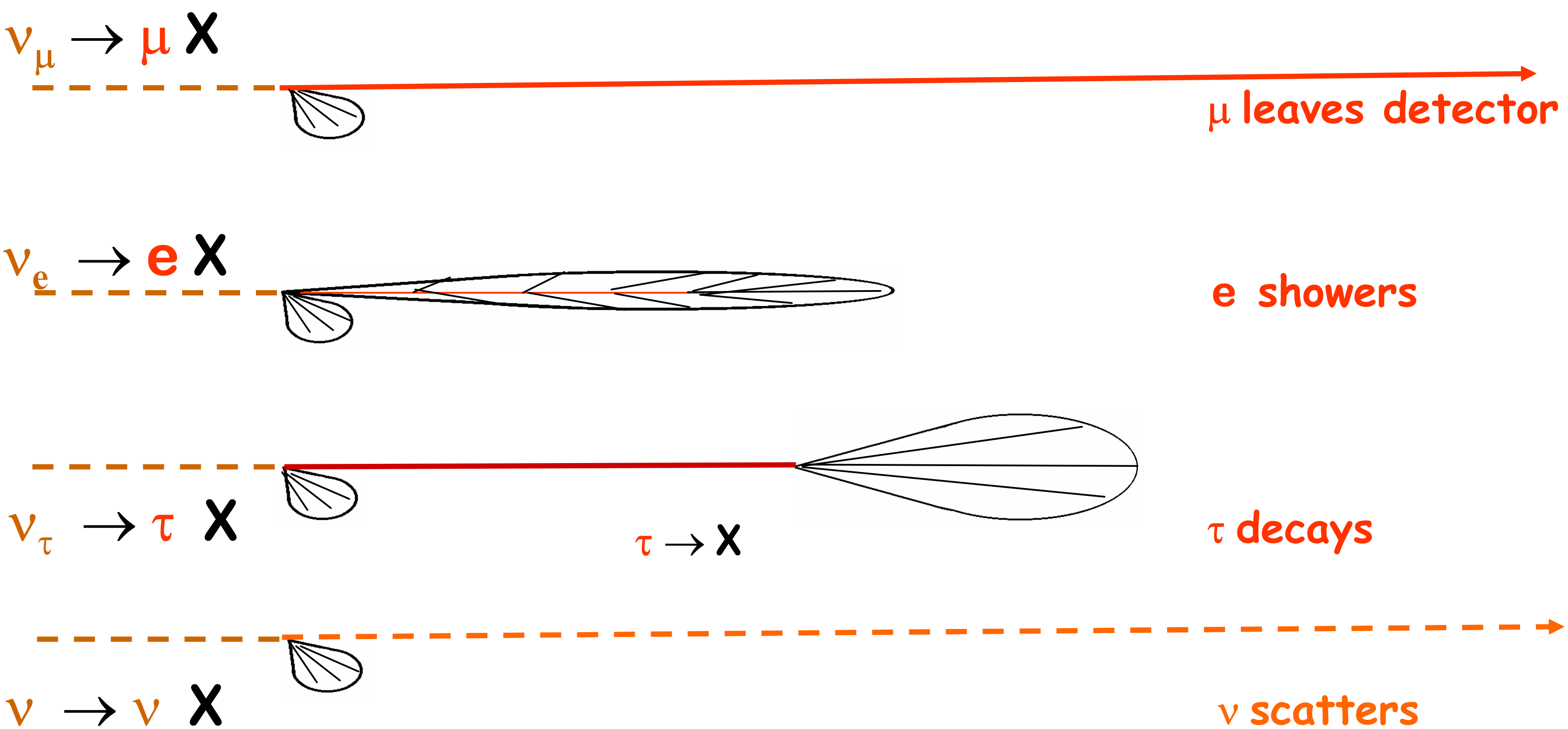

Detectors optimised for $\nu_\mu \rightarrow \mu$ **X,** other modes have lower detection efficiency

Neutrino Telescope Projects

ANTARES La-Seyne-sur-Mer, France
(NEMO Catania, Italy)

BAIKAL: Lake Baikal, Siberia

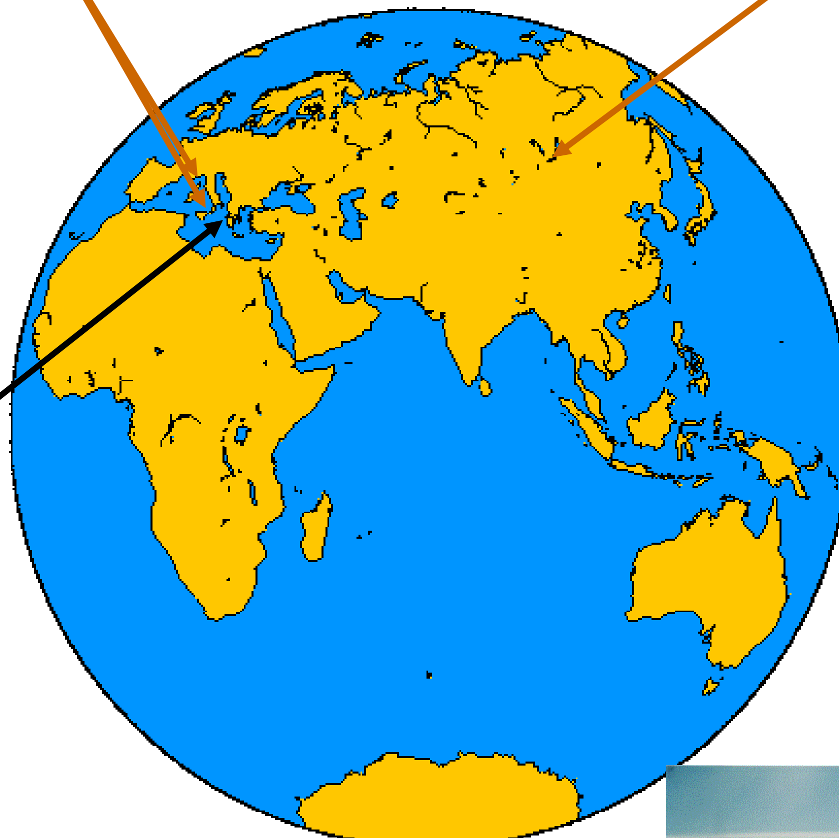

NESTOR : Pylos, Greece

AMANDA, South Pole, Antarctica

Principle of H_2O Cherenkov Neutrino Astronomy

Muon track direction from arrival time of light
Neutrino direction: $\Delta(\theta_\nu - \theta_\mu) \approx 0.7^o / E^{0.6}(TeV)$
Muon energy from energy loss and range

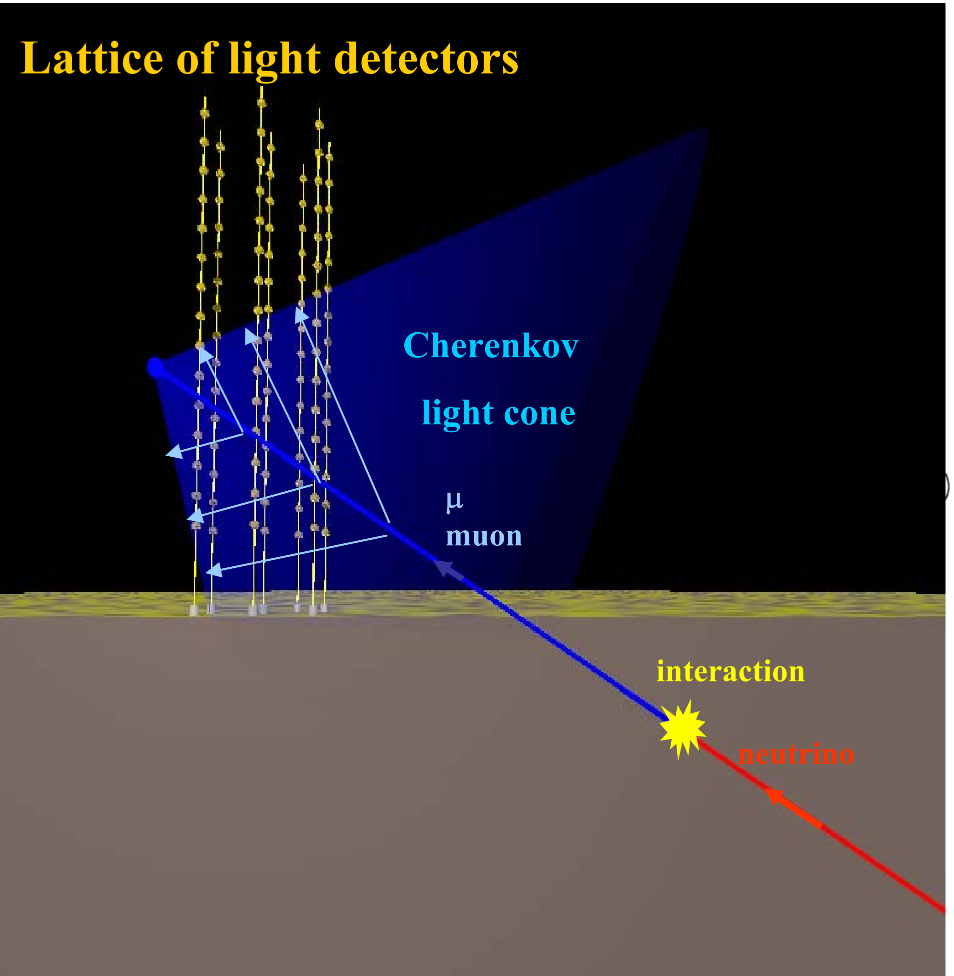

Sky map of origins of neutrinos (Galactic co-ordinate system)

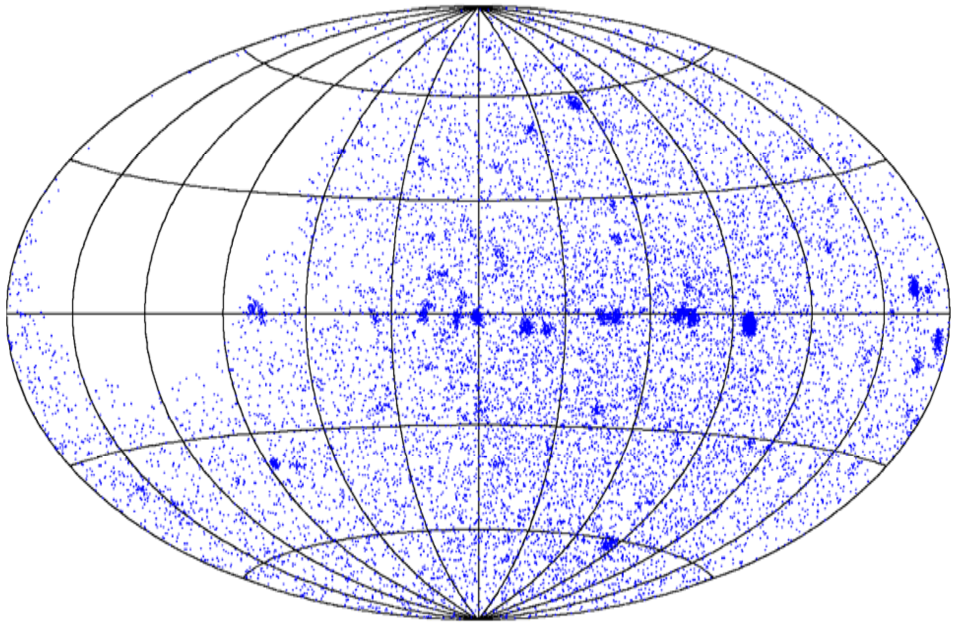

Baikal

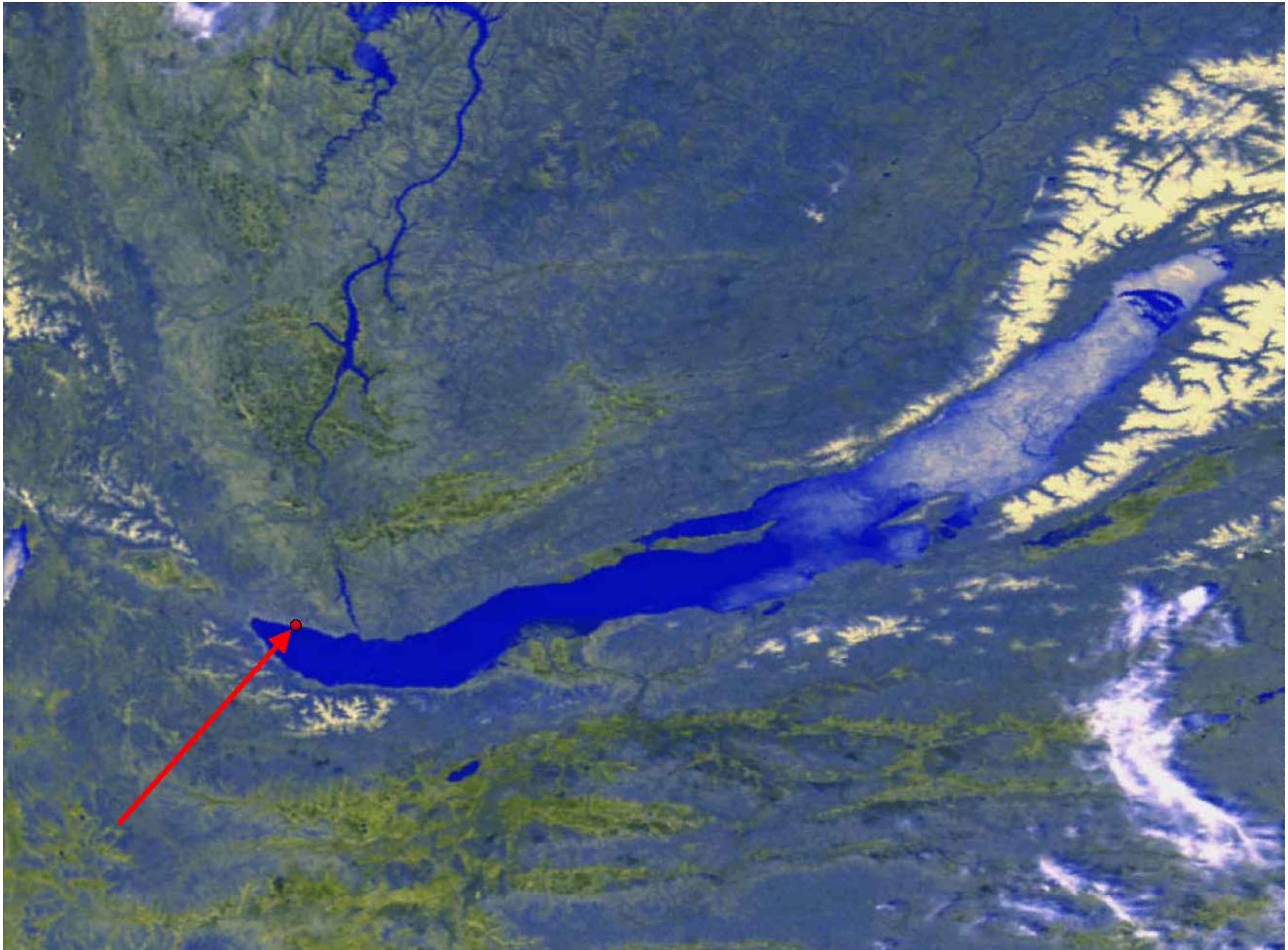

The Site

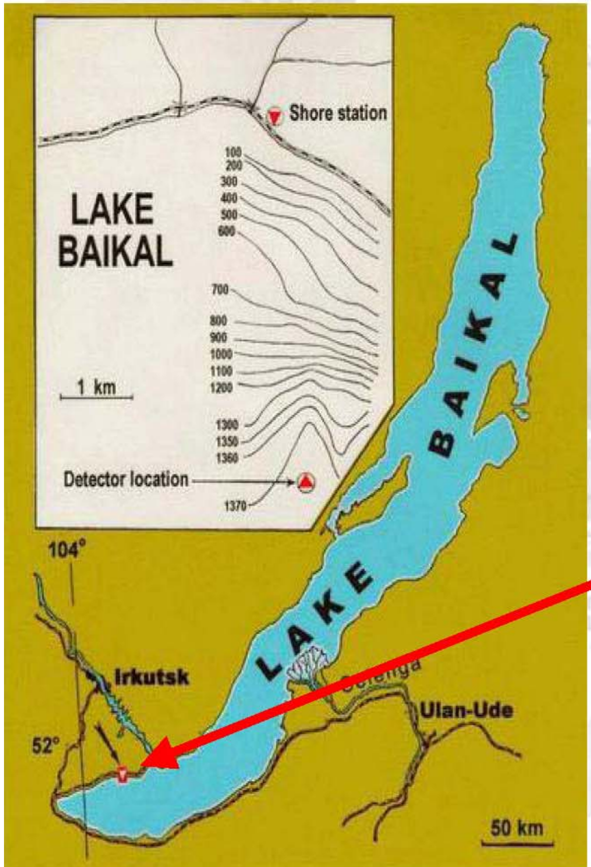

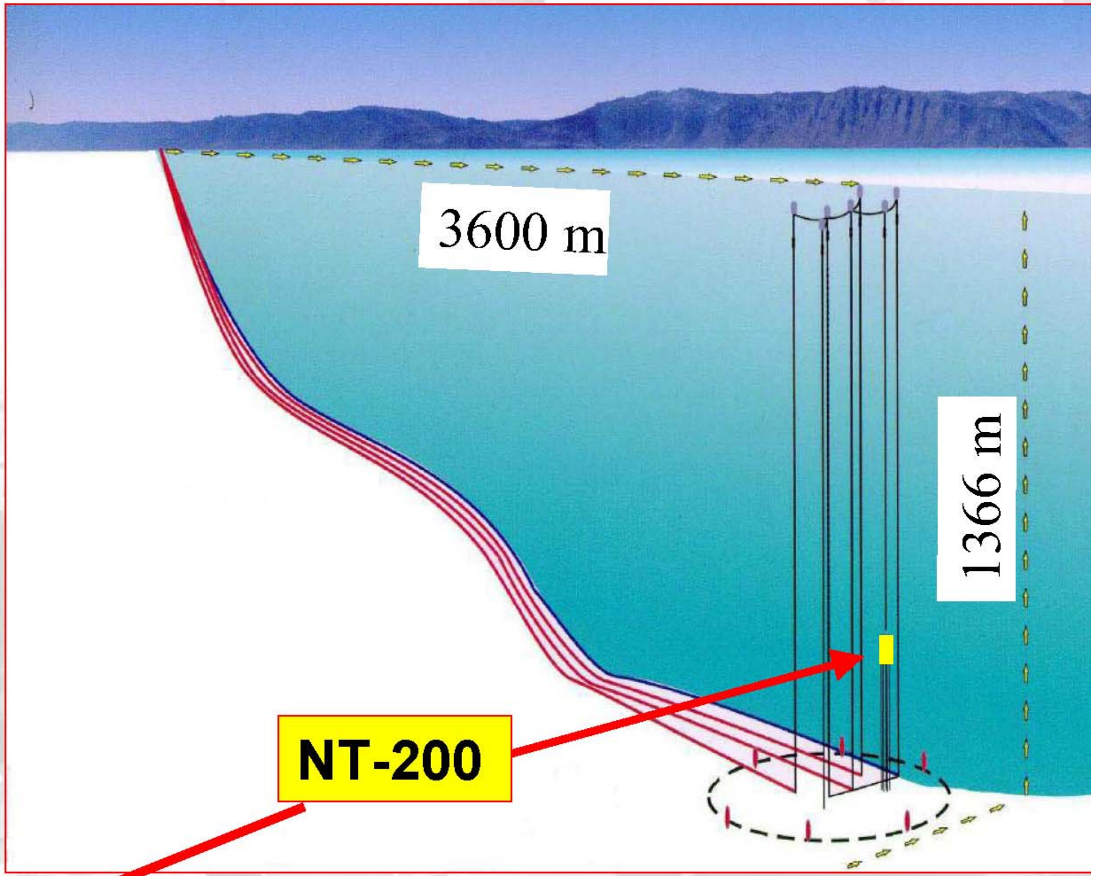

- 4 cables x 4km to shore.
- 1070m depth

Baikal

- Winches used for deployment operations →

Baikal - Optical Properties

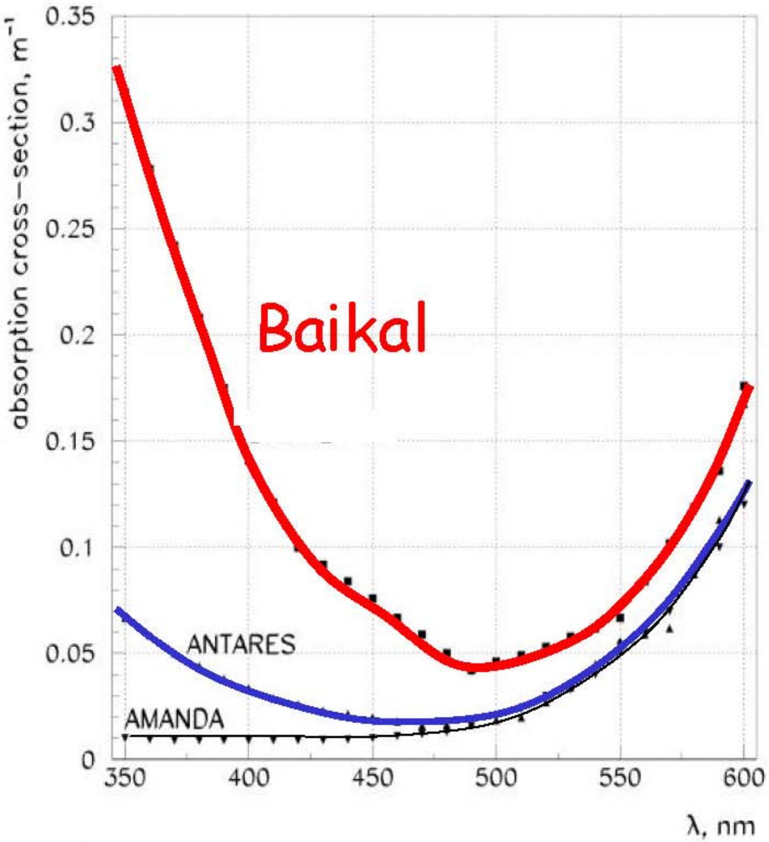

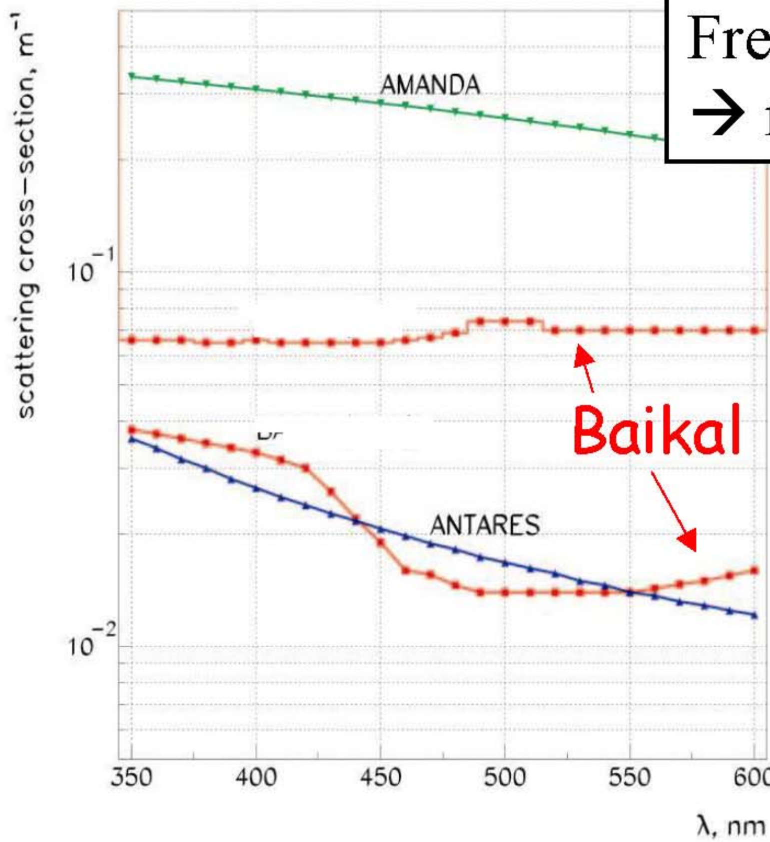

FreshWater
→ no K40 BG

Abs. Length: 22 ± 2 m

In-situ measurements

Scatt. Length (geom) ~ 30-50 m
⟨cos Θ⟩ ~ 0.85-0.9

Rivelatore Baikal

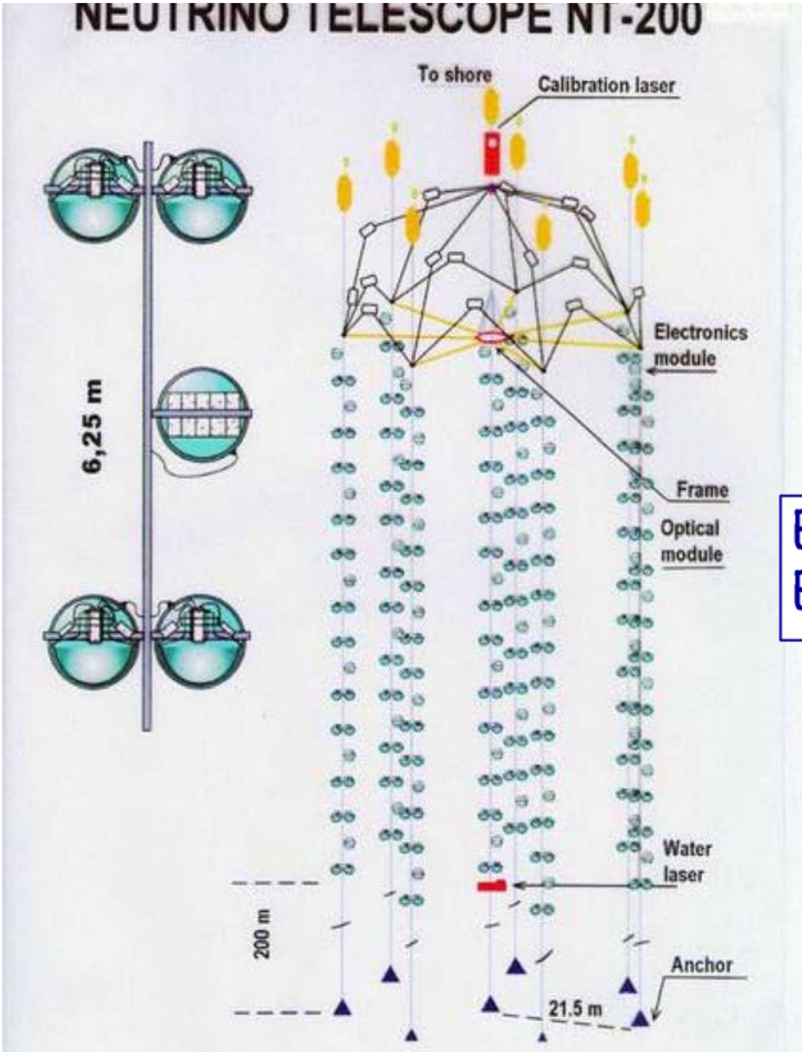

Height x & = 70m x 40m, V=10^5m^3

- 8 strings: 72m height
- 192 optical modules
- pairwise coincidence
  → 96 space points
- calibration with N-lasers
- timing ~ 1 nsec
- Dyn. Range ~ 1000 pe

Effective area: 1 TeV ~2000 m^2
Eff. shower volume: 10TeV ~0.2Mt

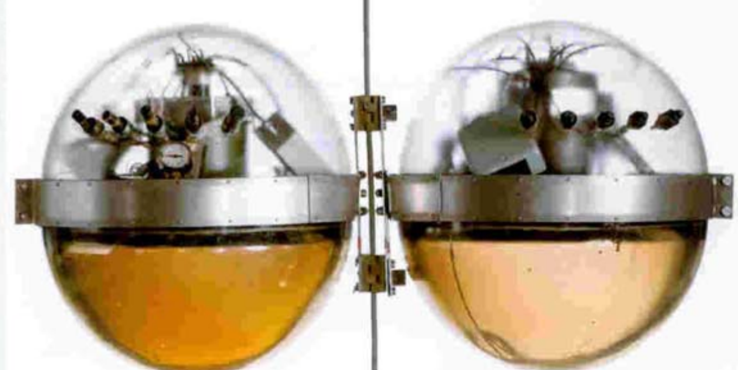

Quasar PMT: d = 37cm

Eventi ν in Baikal

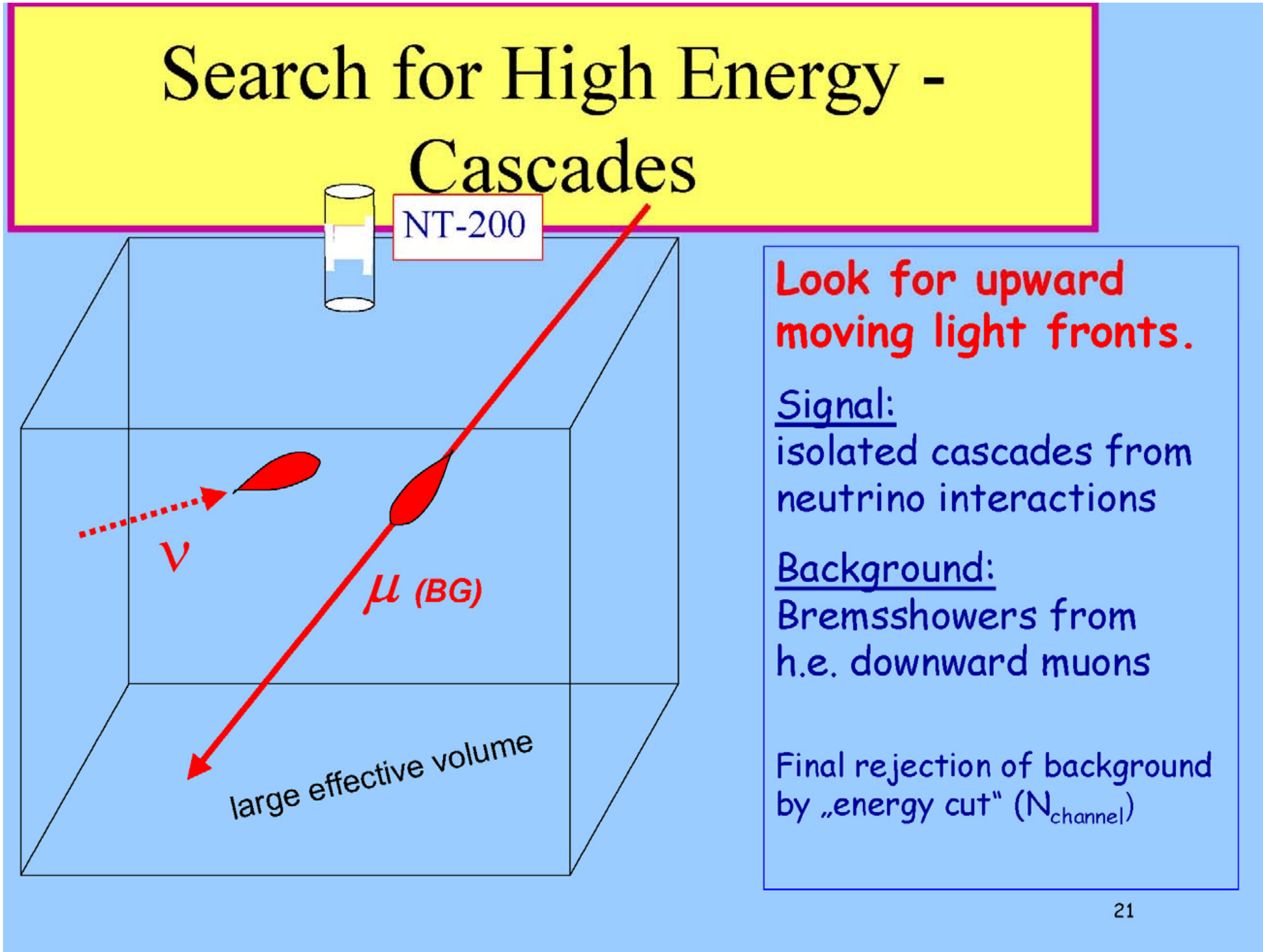

Un evento da neutrino in Baikal

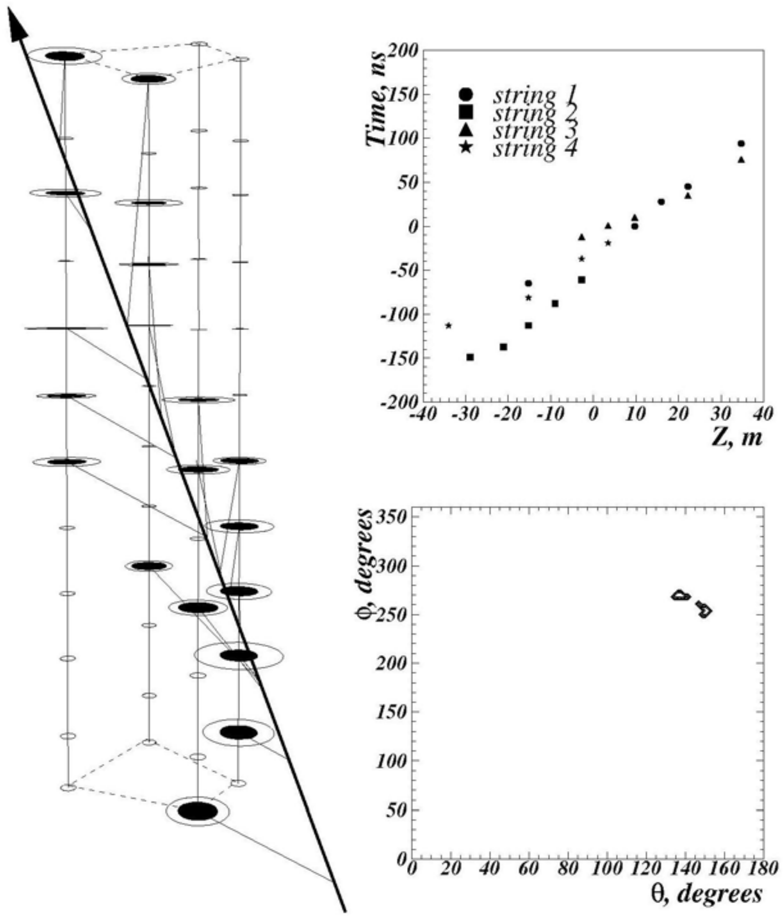

Figure 3: A "gold plated" 19-hit neutrino event. *Left:* Event display. Hit channels are in black. The thick line gives the reconstructed muon path, thin lines pointing to the channels mark the path of the Cherenkov photons as given by the fit to the measured times. The sizes of the ellipses are proportional to the recorded amplitudes. *Top right:* Hit times versus vertical channel positions. *Bottom right:* The allowed θ/ϕ regions (see text).

Amanda

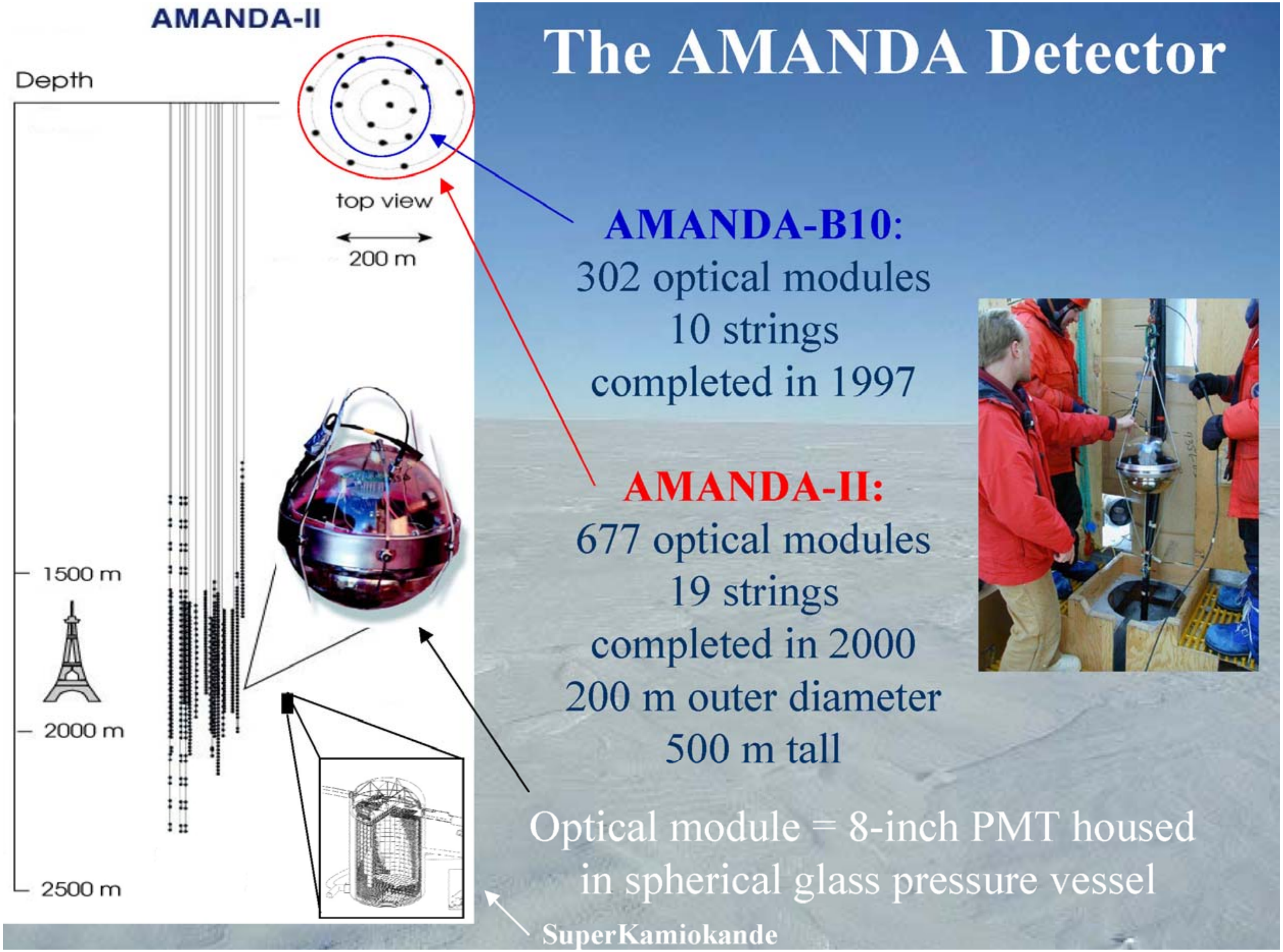
AMANDA-II
Depth
1500 m
2000 m
2500 m
top view
200 m
The AMANDA Detector
AMANDA-B10:
302 optical modules
10 strings
completed in 1997
AMANDA-II:
677 optical modules
19 strings
completed in 2000
200 m outer diameter
500 m tall
Optical module = 8-inch PMT housed
in spherical glass pressure vessel
SuperKamiokande

Amanda

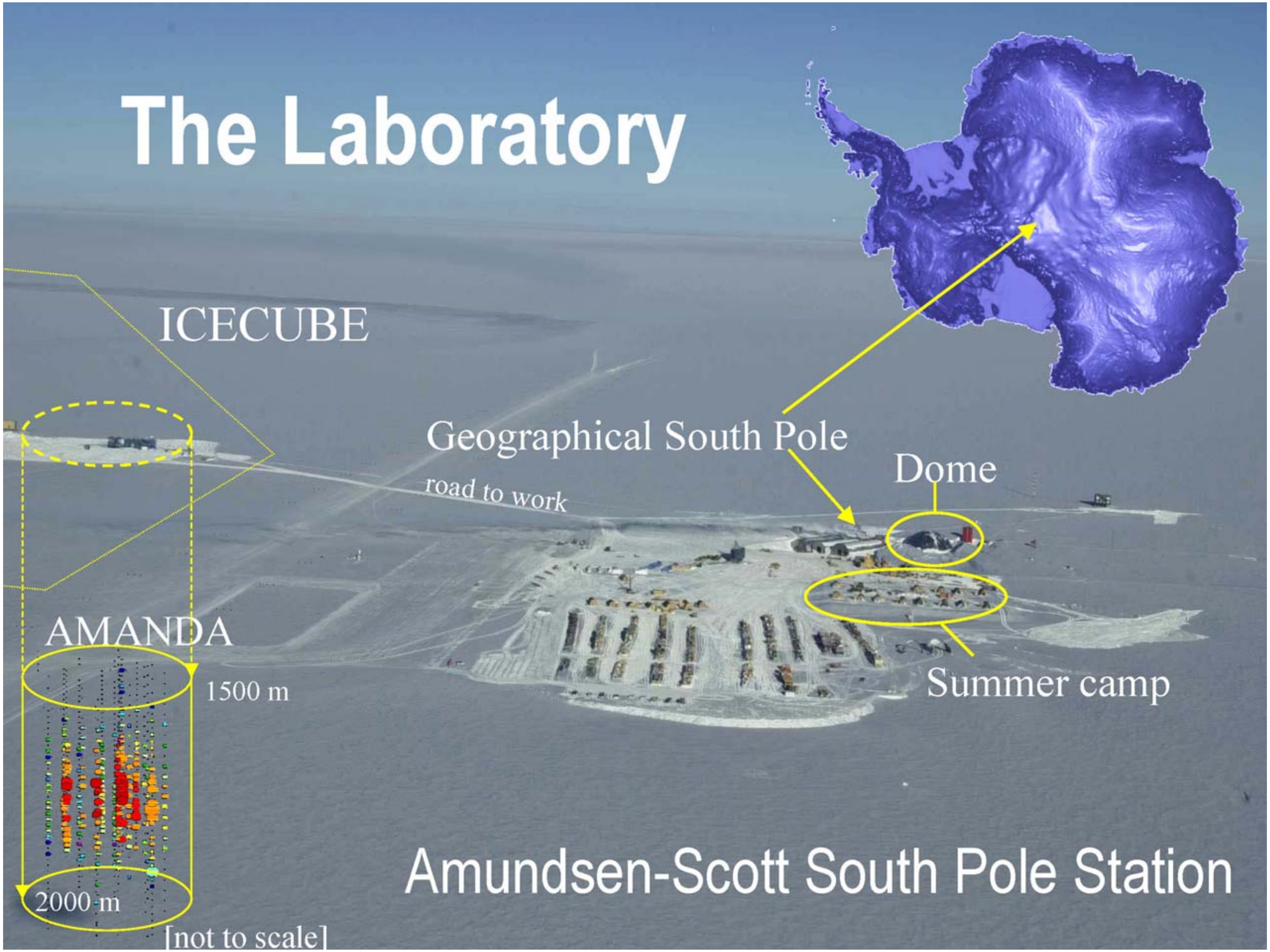

The Laboratory
ICECUBE
Geographical South Pole
road to work
Dome
AMANDA
1500 m
Summer camp
2000 m
[not to scale]
Amundsen-Scott South Pole Station

Amanda

Atmospheric neutrino spectrum

… as a test beam for the AMANDA detector

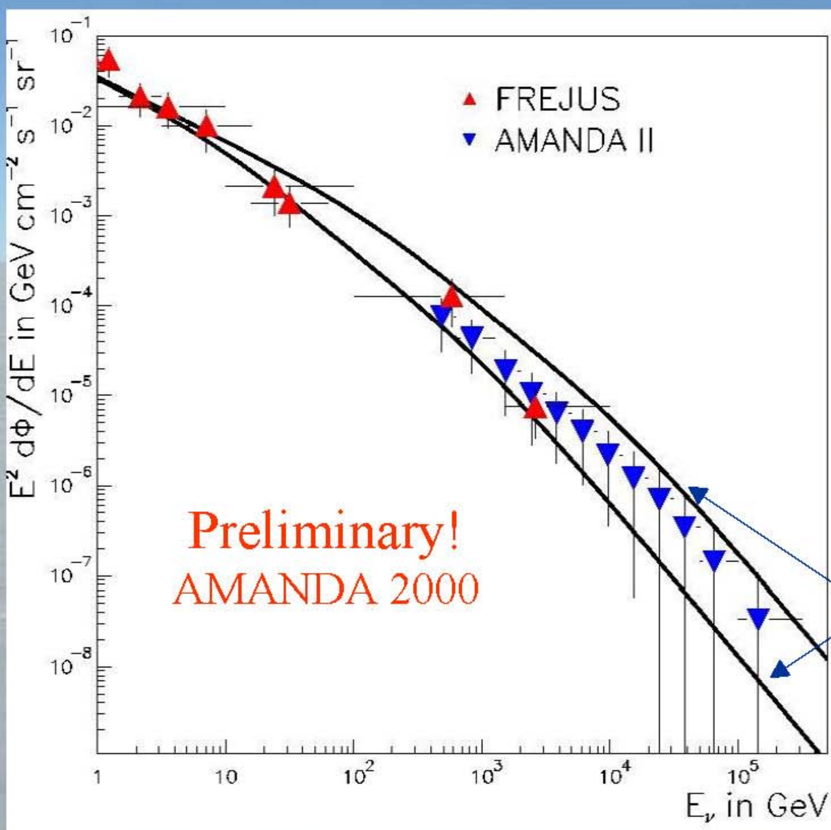

- Background of down-going atmospheric muons $10^6 \times$ more abundant
- Energy reconstruction based on neural network and regularized unfolding
- First energy spectrum > 1 TeV
- Matches lower-energy Frejus data
- Compatible with expectation of atmospheric neutrino flux

Spectrum is used to study excess due to cosmic neutrinos

Amanda

Search for extraterrestrial point sources

→ Look for an excess of up-going muon tracks in particular directions in the sky (sky bins)

- Grid search: sky subdivided into 300 bins (~7°*7°)
- Optimization of cuts in each declination band

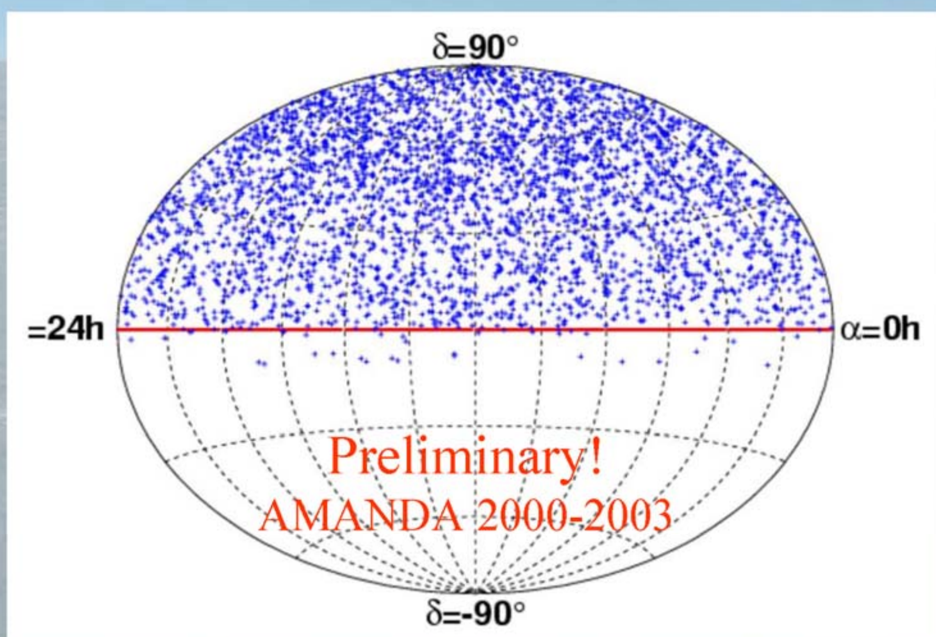

- 3369 neutrino events observed from below the horizon, while 3438 expected from atmospheric neutrino simulation

No clustering observed

⇓

No evidence for point sources

Amanda

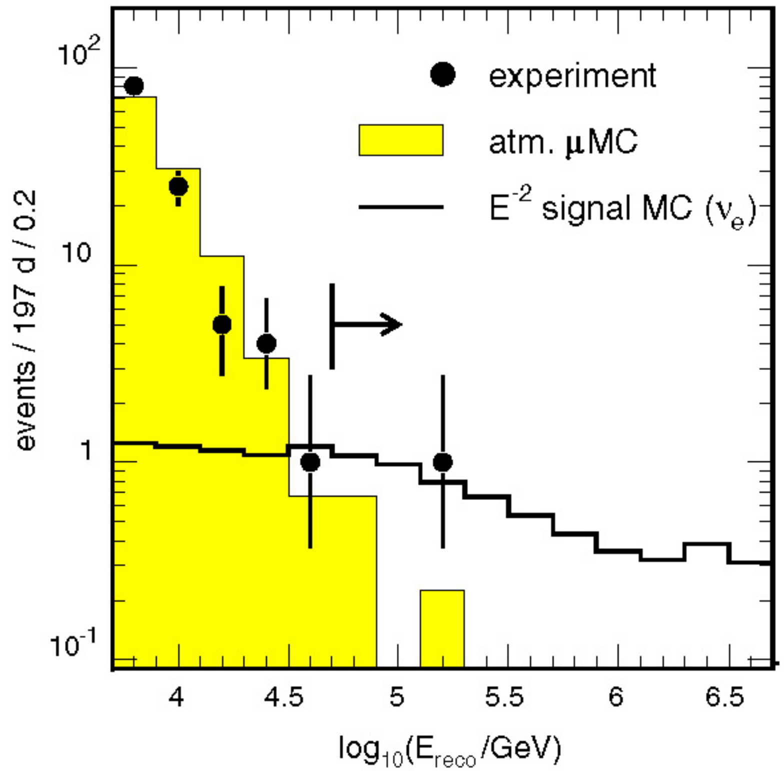

Fig. 3. Distributions of reconstructed energies after all but the final energy cut. Shown are experimental data, atmospheric muon simulation and a hypothetical flux of astrophysical neutrinos. The final energy cut is indicated by the line with the arrow.

Search for extraterrestrial point sources

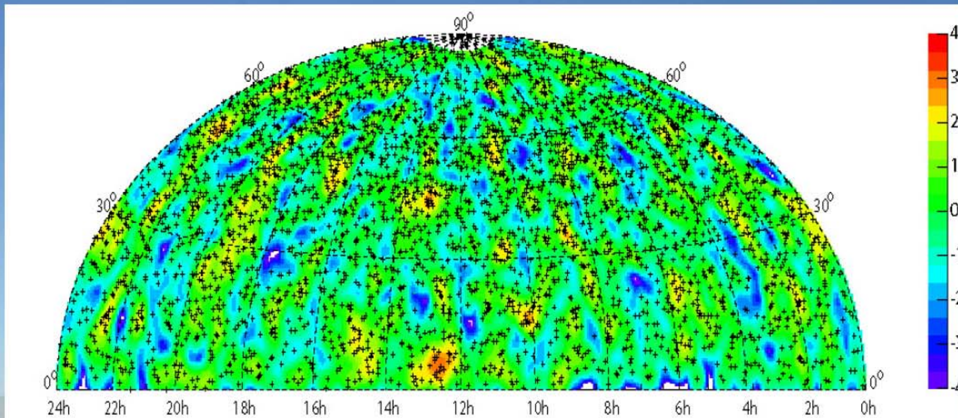

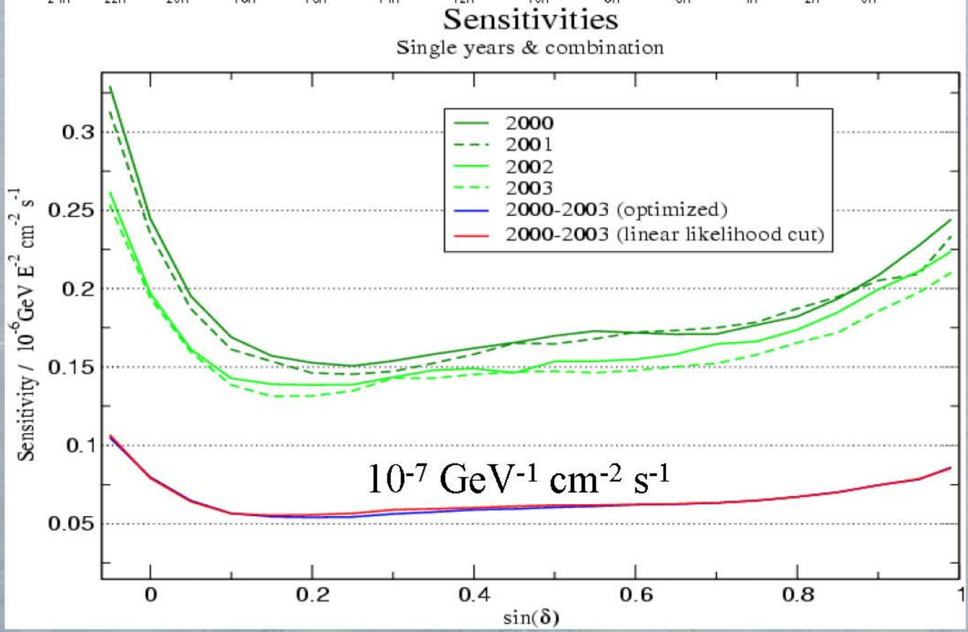

- Significance of local fluctuations compared to expectation of all being atmospheric neutrinos

➔ max 3.4 σ

⇒ compatible with bg fluctuation

- Improved sensitivity for full data set (2000-2003)
- 807 days of live time

published results
Data 1997 : Ap.J. 583, 1040 (2003)
Data 2000 : PRL 92, 071102 (2004)

Amanda

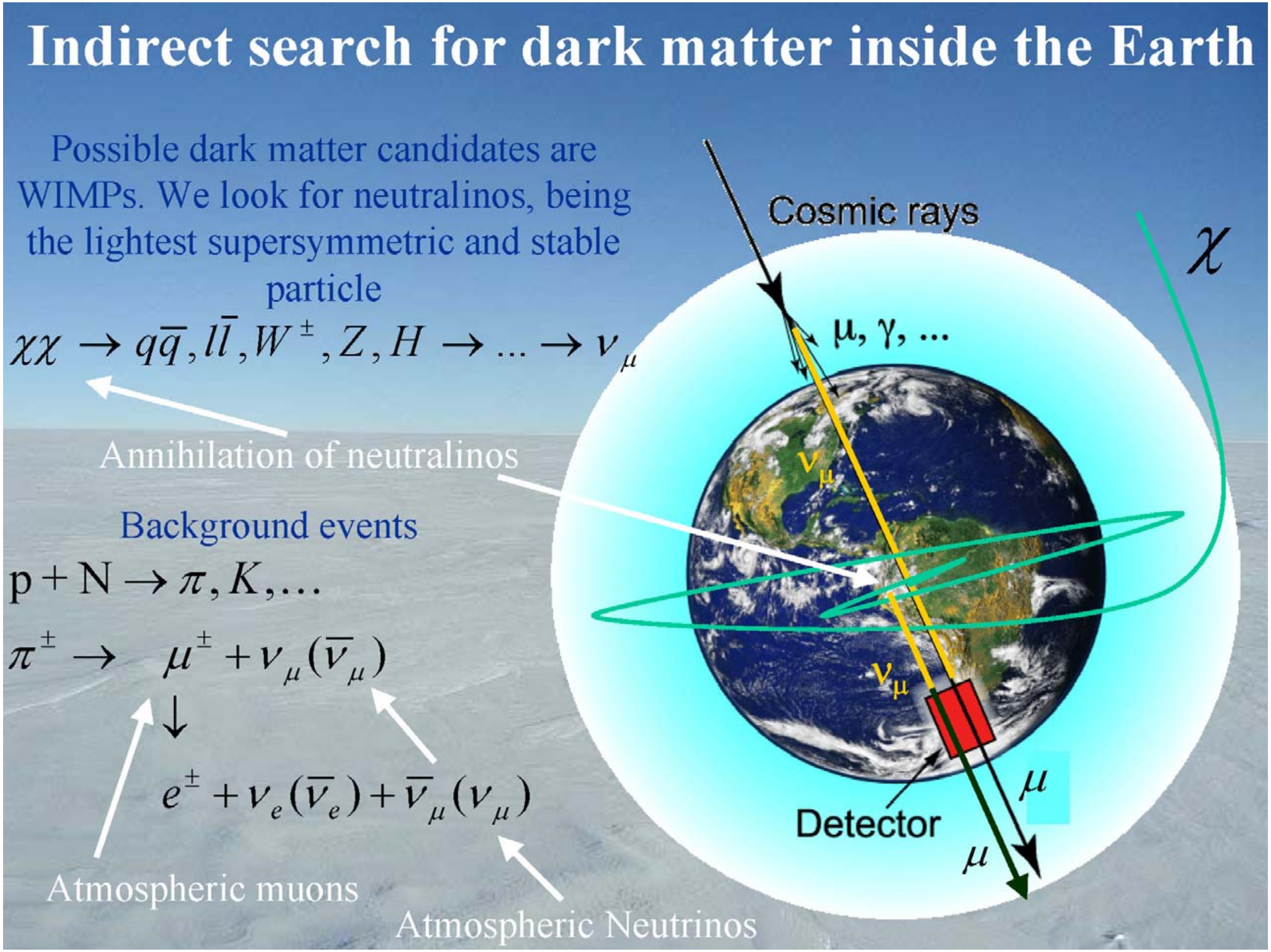
Indirect search for dark matter inside the Earth
Possible dark matter candidates are WIMPs. We look for neutralinos, being the lightest supersymmetric and stable particle
$\chi\chi \to q\bar{q}, l\bar{l}, W^{\pm}, Z, H \to \dots \to \nu_{\mu}$
Annihilation of neutralinos
Background events
$p + N \to \pi, K, \dots$
$\pi^{\pm} \to \mu^{\pm} + \nu_{\mu}(\bar{\nu}_{\mu})$
$\downarrow$
$e^{\pm} + \nu_e(\bar{\nu}_e) + \bar{\nu}_{\mu}(\nu_{\mu})$
Atmospheric muons
Atmospheric Neutrinos
Cosmic rays
χ
μ, γ, ...
ν_{μ}
ν_{μ}
Detector
μ
μ

ANTARES Collaboration

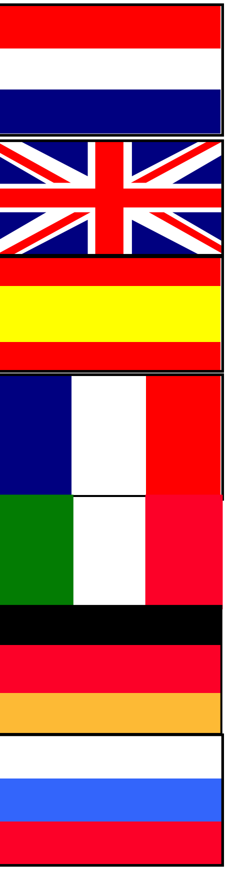

University of Sheffield
University of Leeds
IFIC, Valencia
CPPM, Marseille
DSM/DAPNIA/CEA, Saclay
C.O.M. Marseille
IFREMER, Toulon/Brest
LAM, Marseille
IReS, Strasbourg
Univ. de H.-A., Mulhouse
ISITV, Toulon
LOV Villefranche
INFN+University of Bari
INFN+University of Bologna
INFN+University of Catania
INFN-LNS Catania
INFN+University of Pisa
INFN+University of Rome
INFN+University of Genova
University of Erlangen
ITEP, Moscou

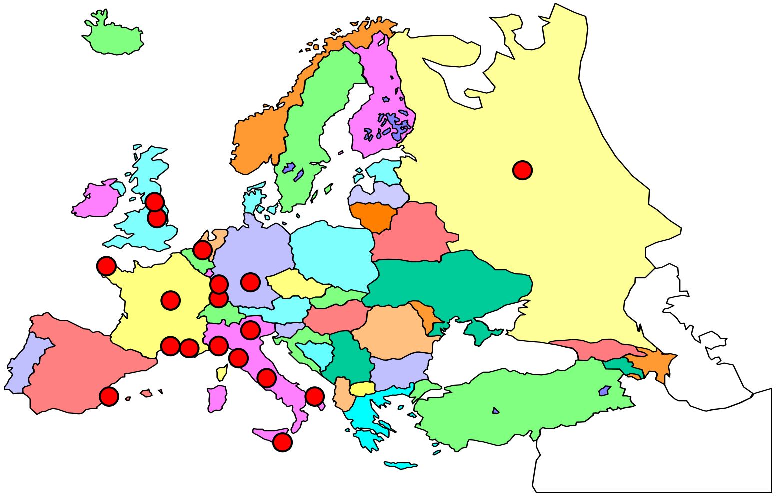

ANTARES test sites

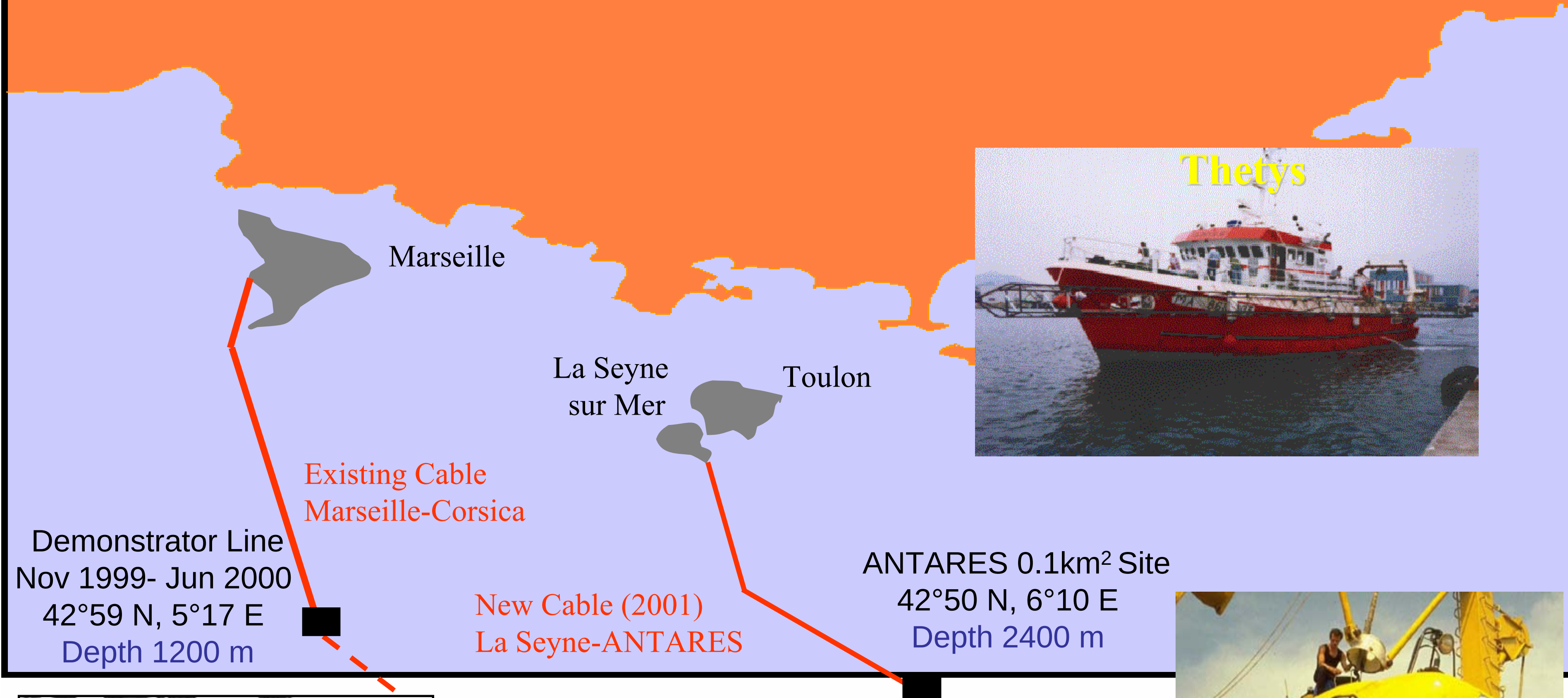

~ 40 deployments and recoveries of test lines for site exploration.

Site Explorations

Tests: demonstrator line

November 1999–June 2000

350 m long; immersed at 1200 m depth equipped with 7 PMTs

Main results:

acoustic positioning system accuracy: 5 cm

atmospheric muon zenith distribution

data to shore system checked

Measurements of water optical Properties:

- Absorption length = 60 m

- Effective scattering length = 265 m

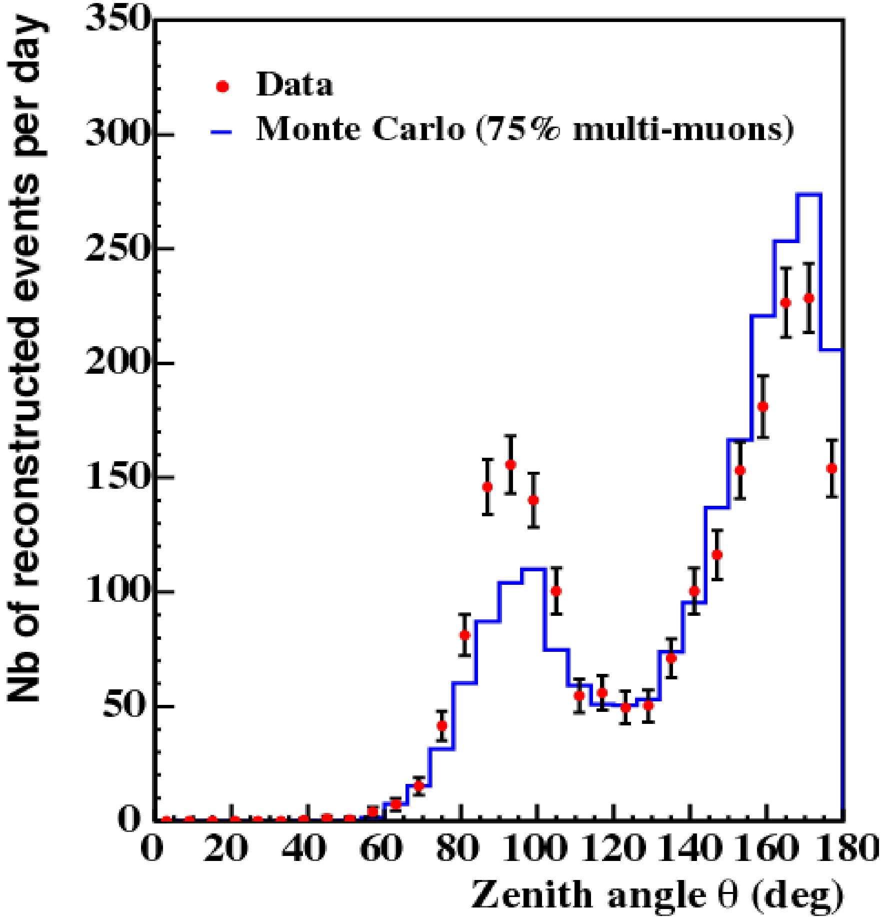

50000 events with 7-fold coincidences

Biofouling

Optical Backgrounds

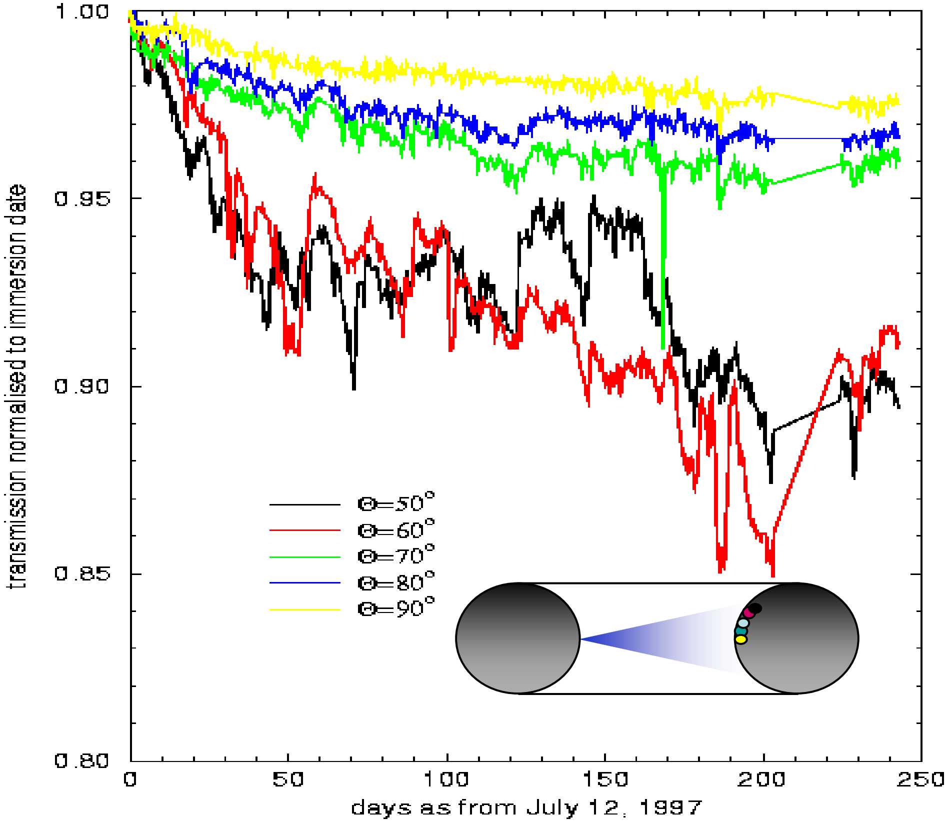

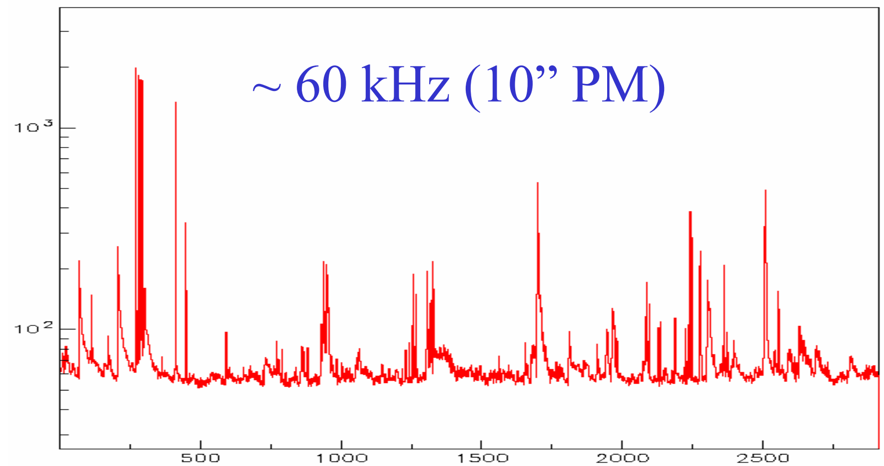

Short bursts (bioluminescence) over a continuous background (^{40}K).

~5% of time a PMT is unusable

For θ > 90º transmission loss <1.5% in 1 yr (and saturates)

Bioluminescent bacteria

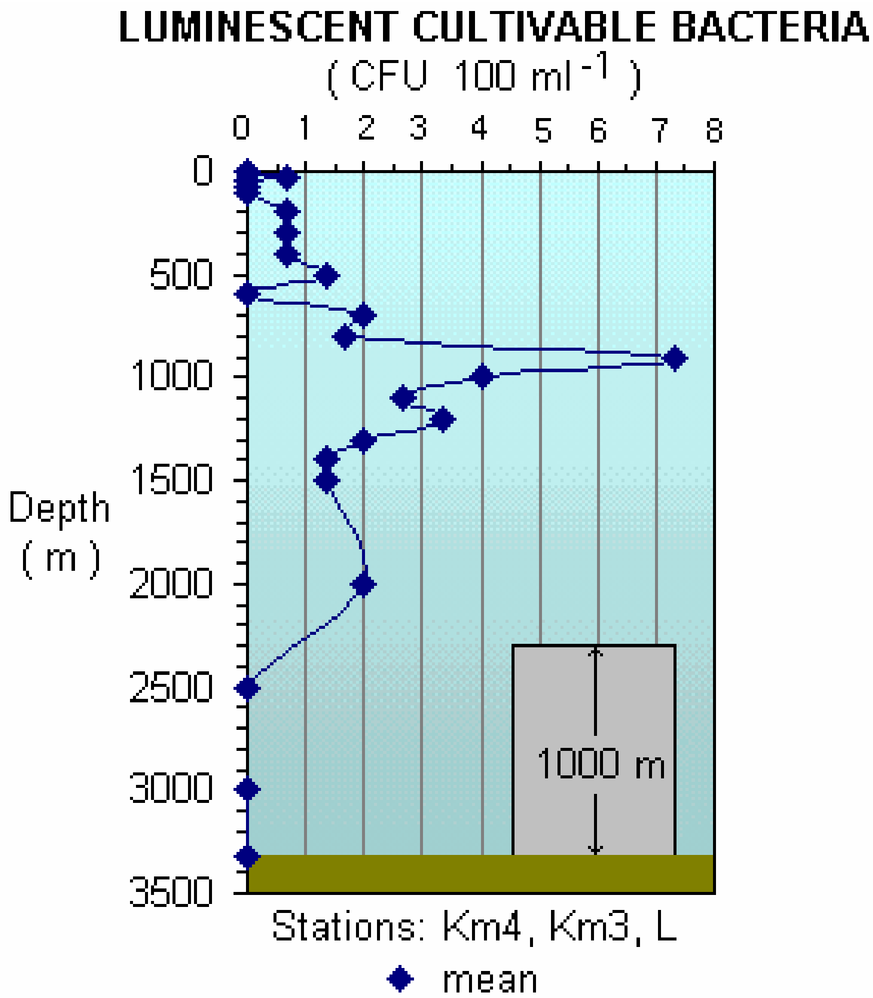

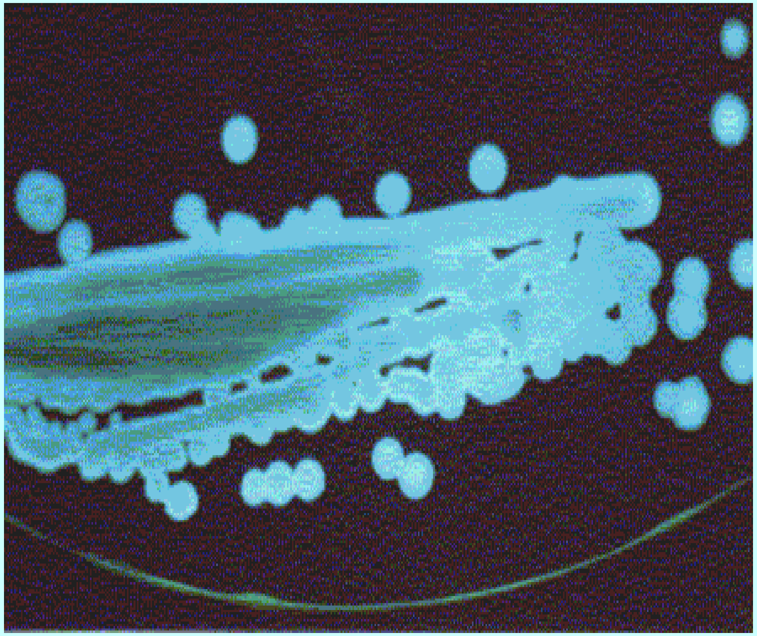

Bioluminescent bacteria on SWC

ANTARES Detector

12 strings
75 10" PM's per string (PM's at 45^0 wrt sea-bed)
Arranged in groups of 5 triplets (storeys) per section
5 sections/string

Storeys are 14.5 m apart. Interconnected by electro-optical cables providing: power, control signals, data transmission
Local Control Modules (LCM) connected to String Control Module (SCM) (Bottom of string)
SCM connected to Junction Box
JB connected to submarine cable

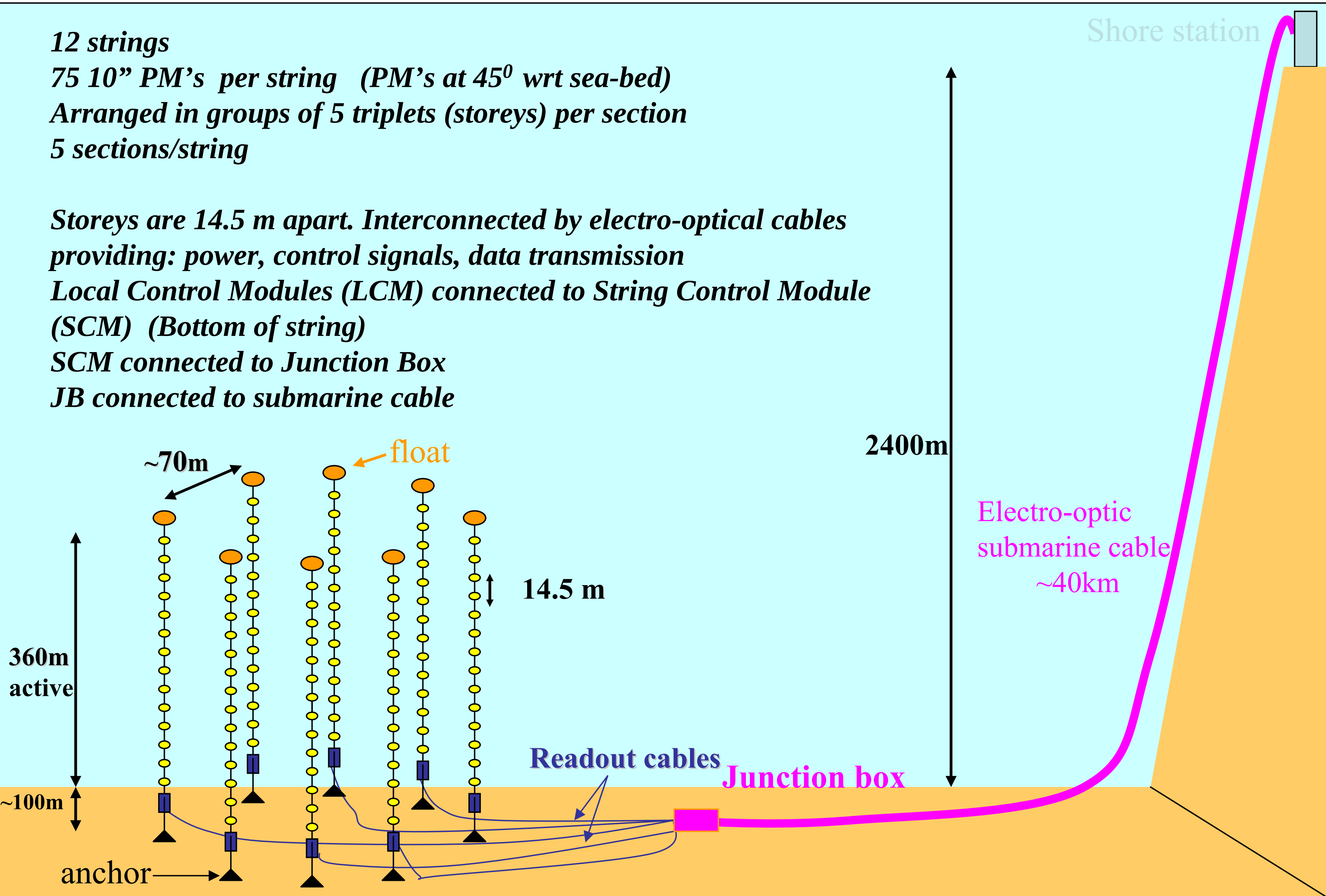

Detector layout

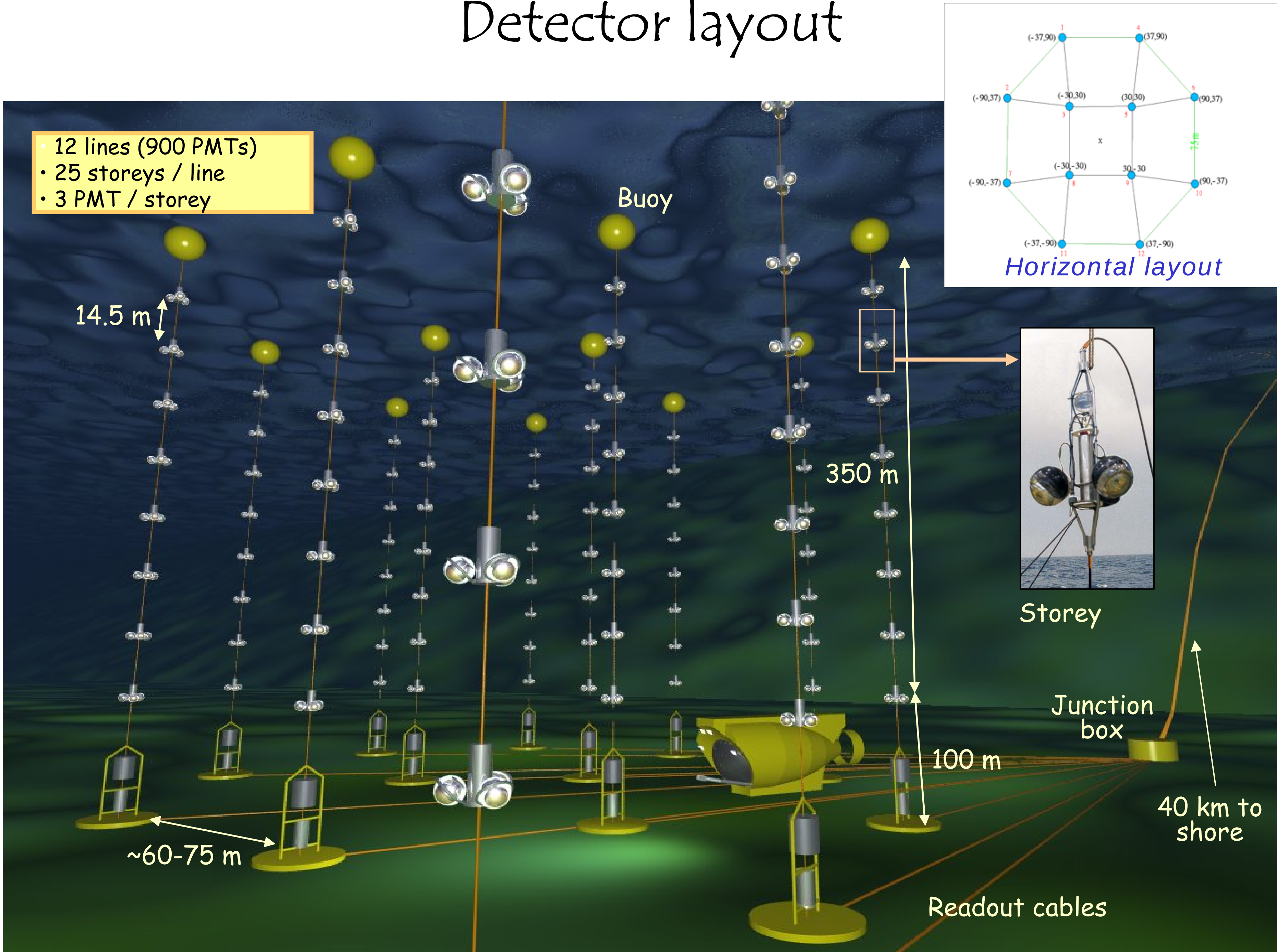

Detector design

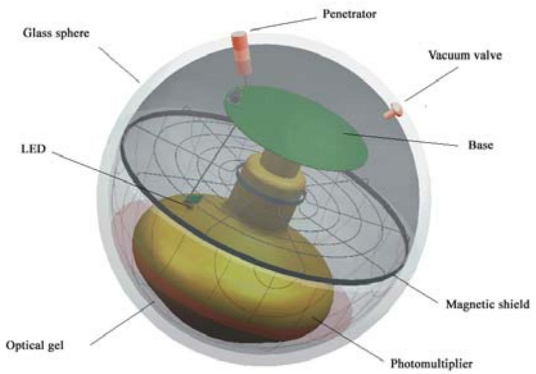

The Optical Module contains a 10'' PMT and the associated electronics.
An internal LED will monitor the transit time of the PMT.

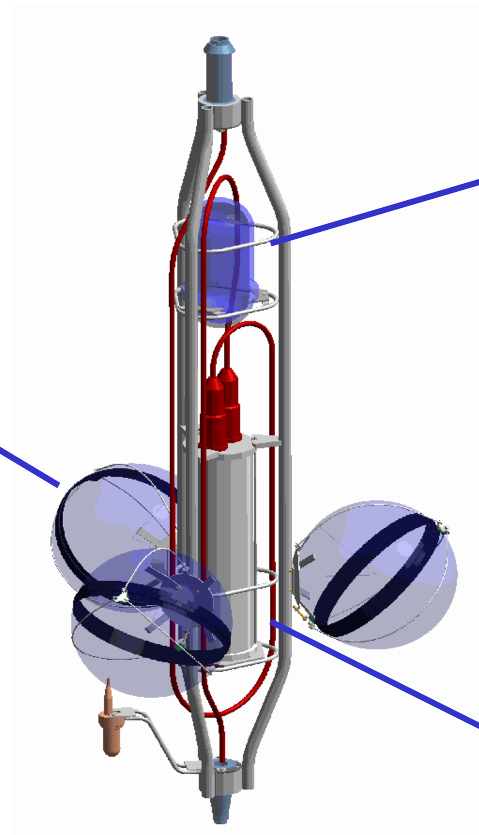

The storey

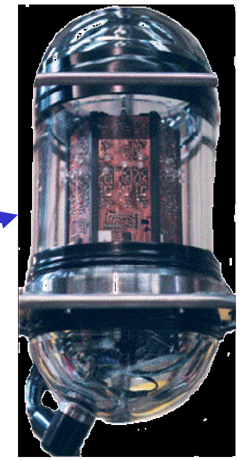

The Optical Beacons will allow the timing calibration of the detector with external sources (blue LEDs)

The Local Control Module processes PMT signals. The electronics is housed in a Ti cylinder.

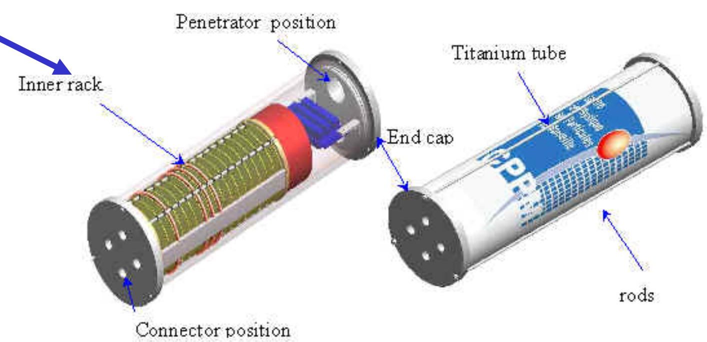

Prototype Line ready: Nov 2002

Line Deployment 0.1km^2 Detector

Storeys deployed two by two

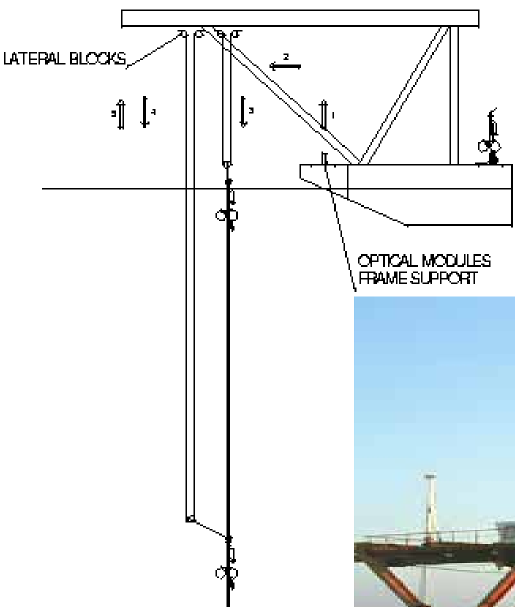

Storeys stored on deck of Castor

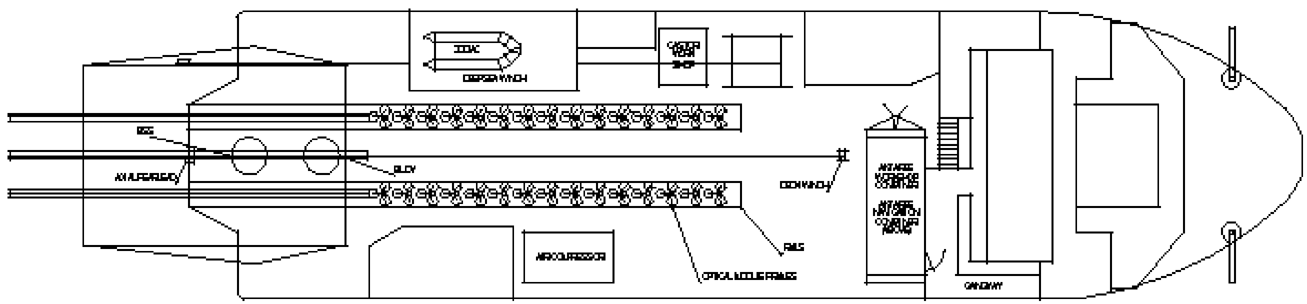

Nautile

Deployment of Junction Box , Dec 2002

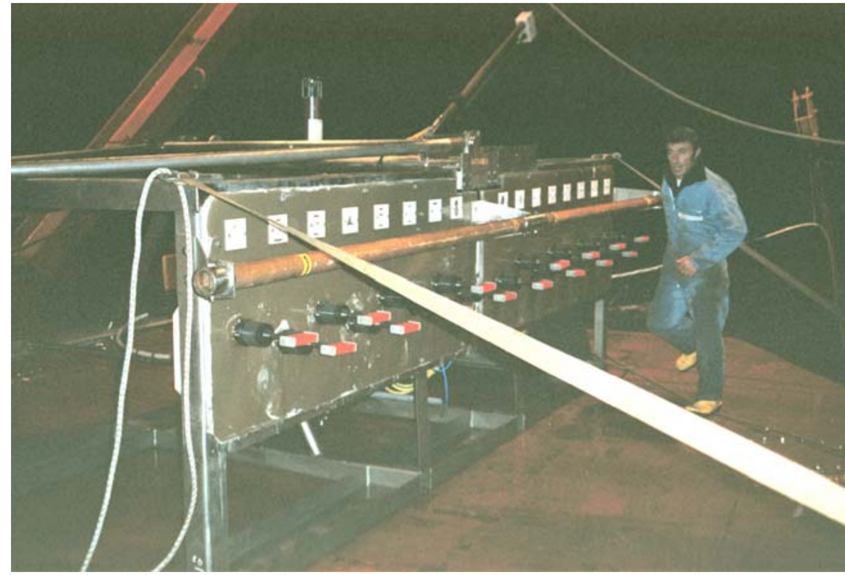

Submarine cable connection

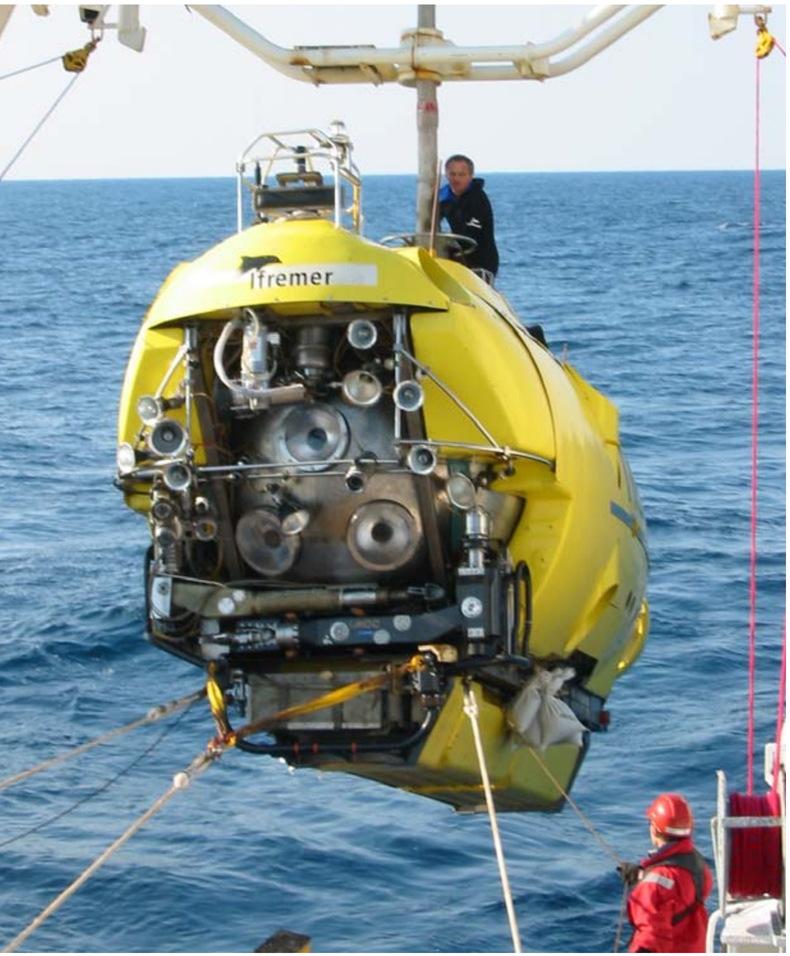

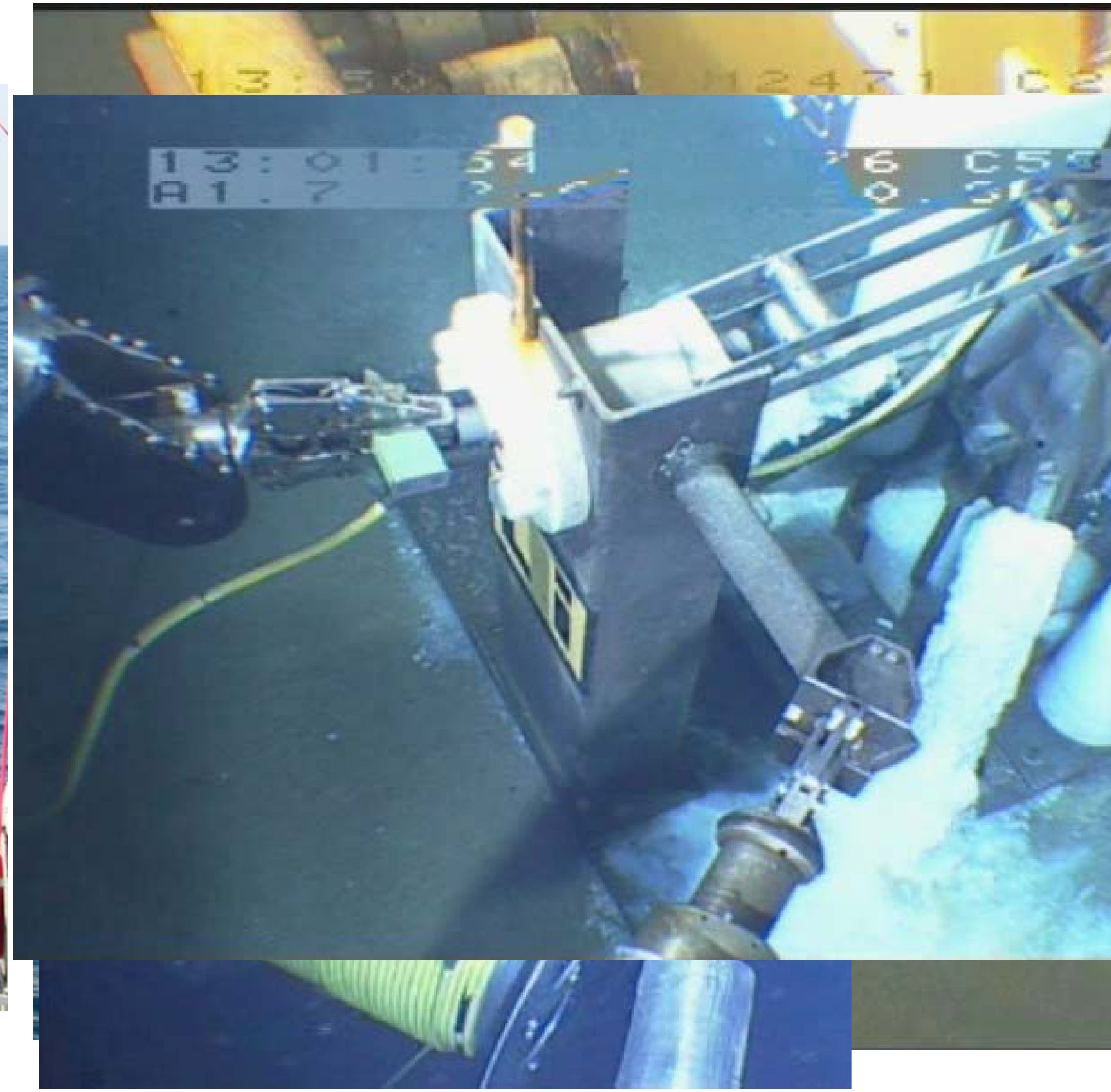

Current layout

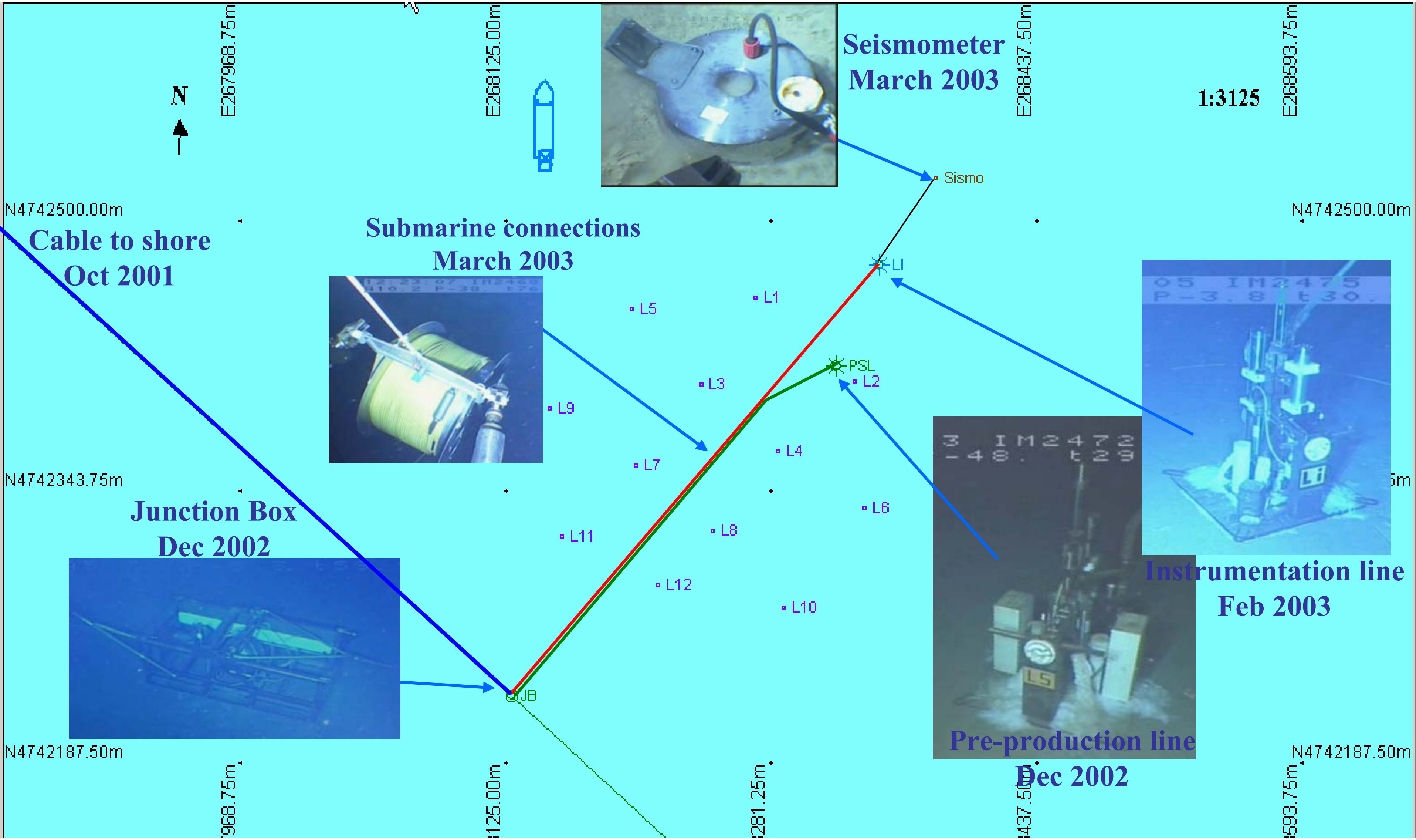

Clock time reference system

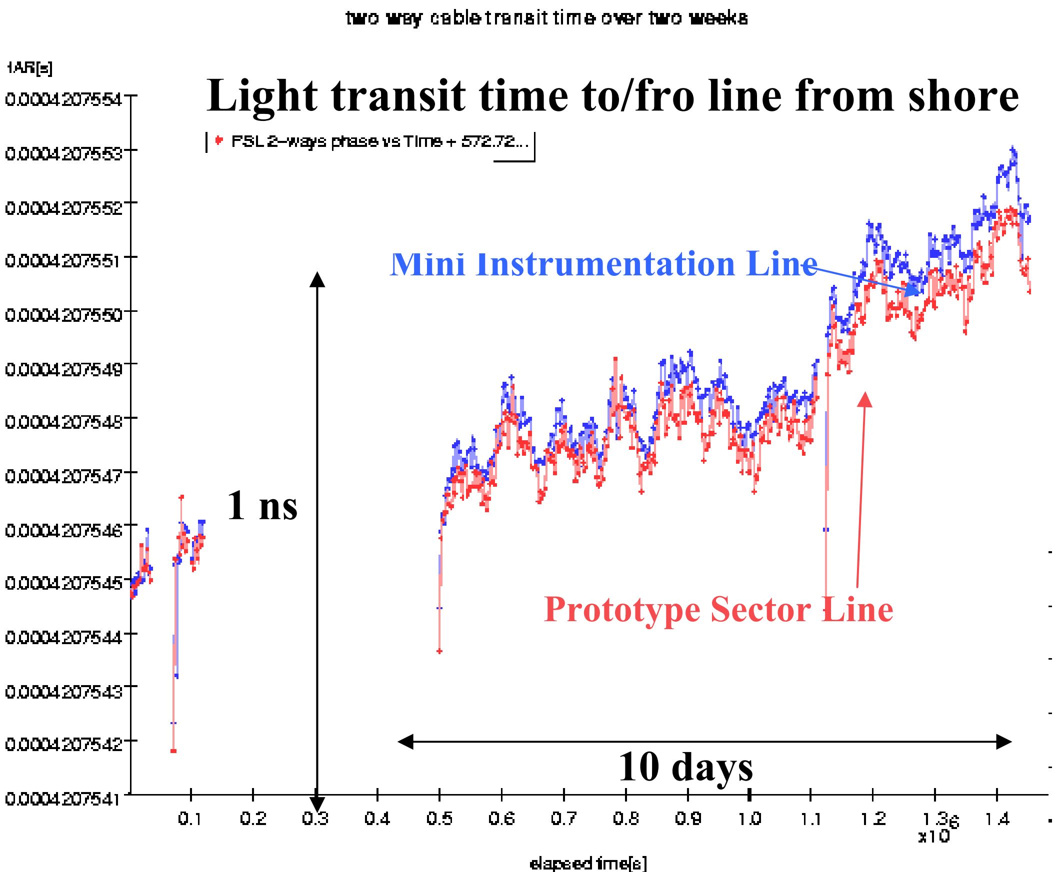

Difference in transit times for two lines

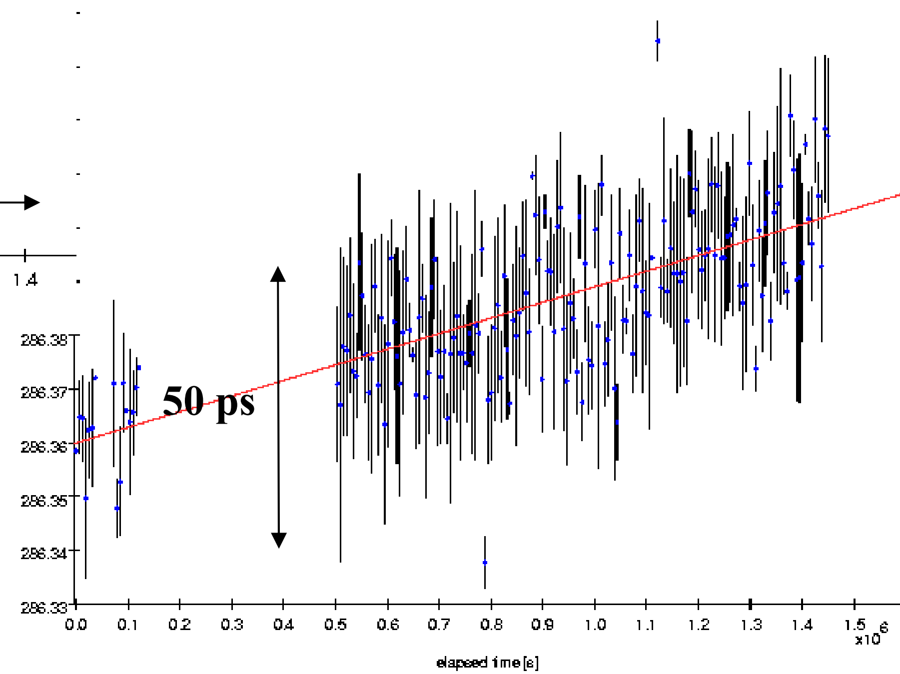

Inertial water motion

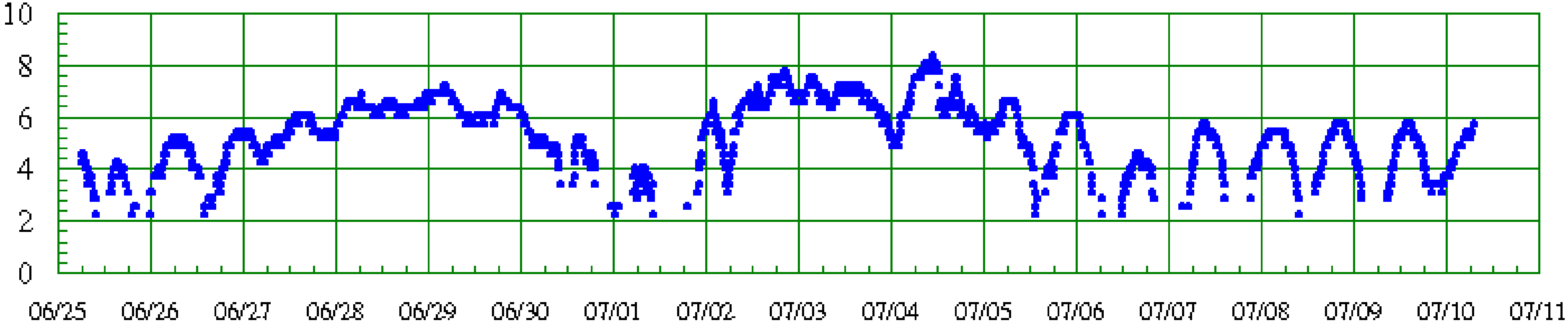

Coriolis effect

$\nu = 2\ \omega \sin\phi$ with $\phi = 42^o$ → **T=18 hr**

where ω is $2\pi/24$ hr

Correlation with current speed

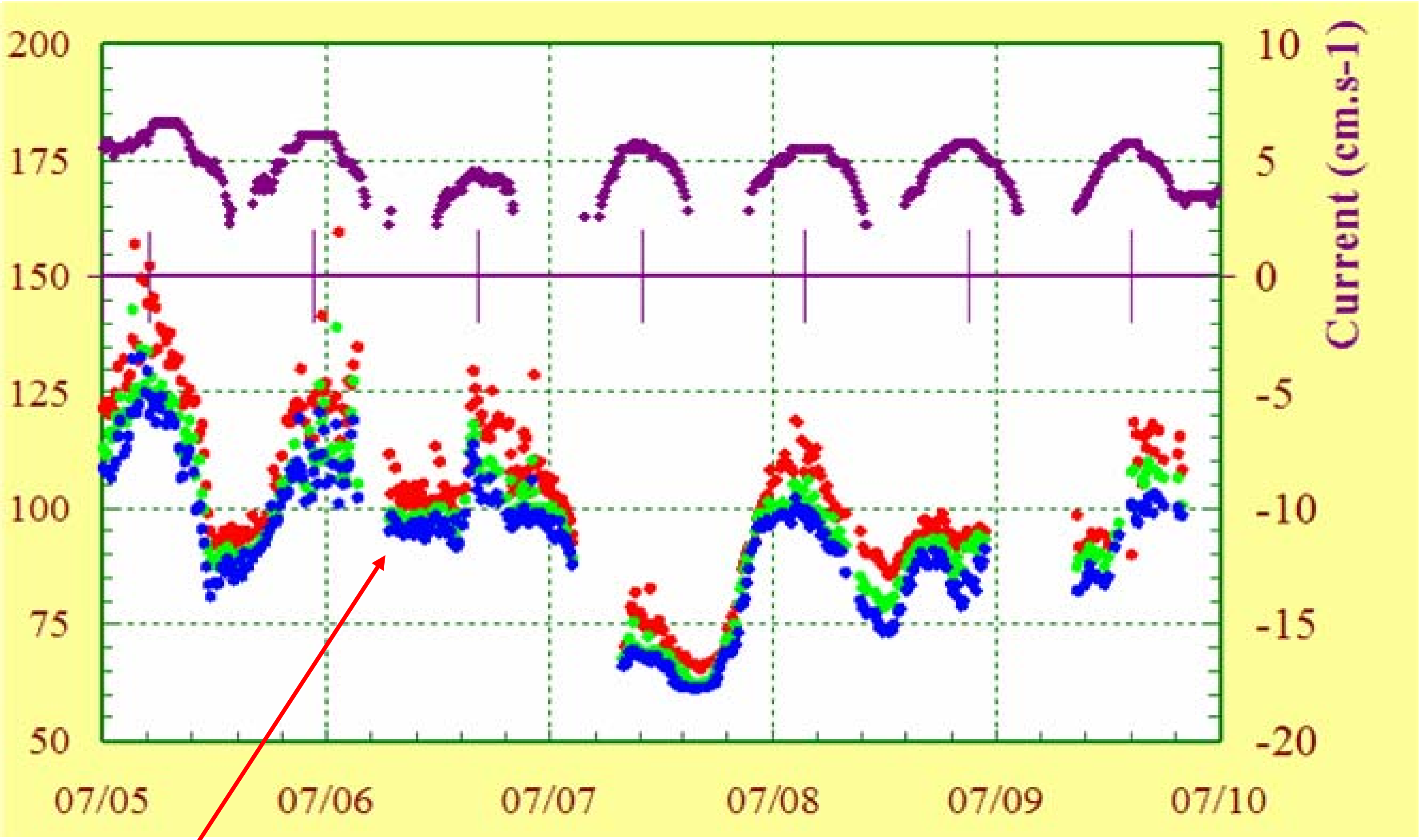

Attvita' ottica dovuta a bioluminescenza

Correlation plot

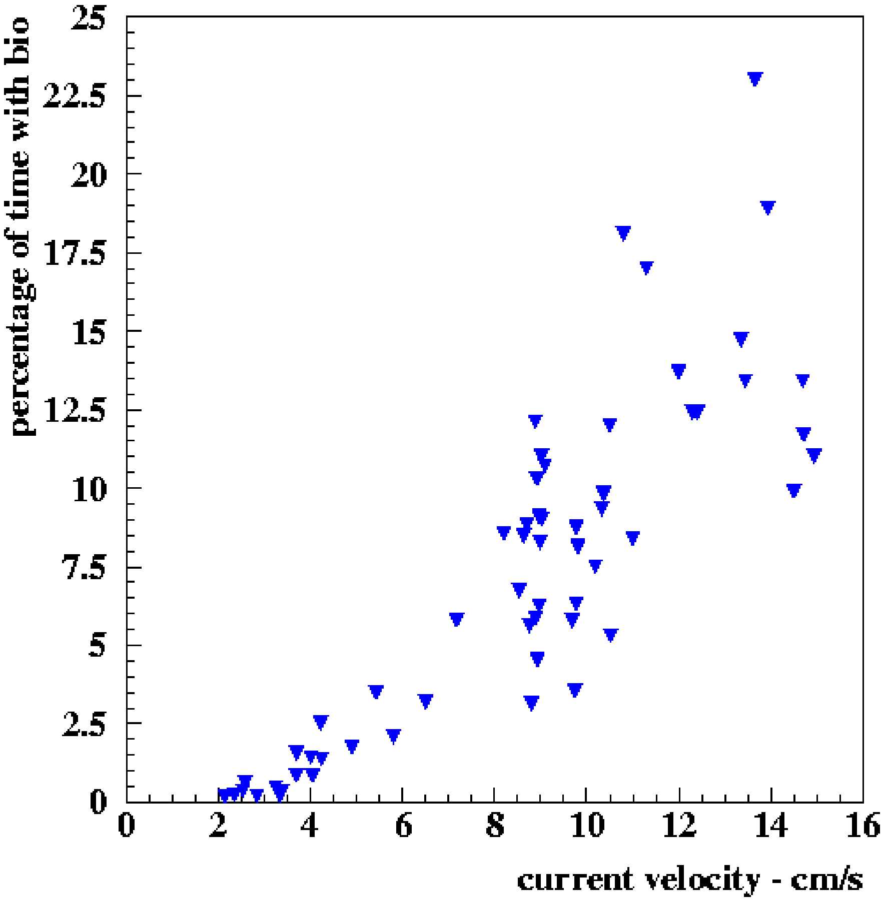

Expected performance

Angular resolution

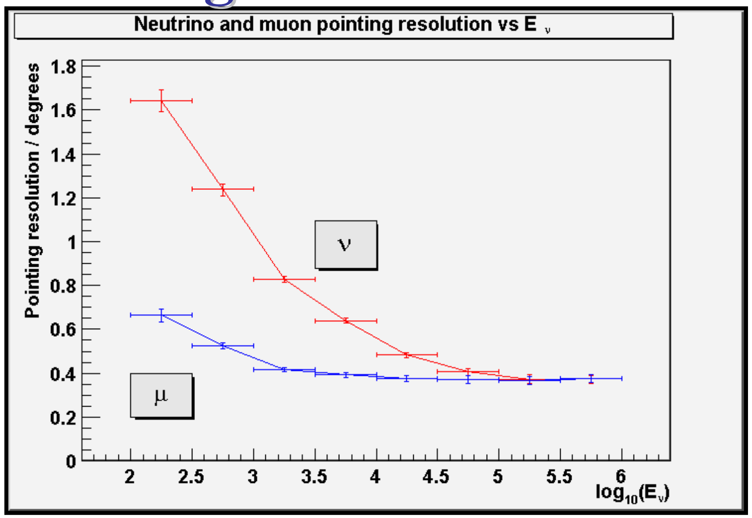

Energy resolution

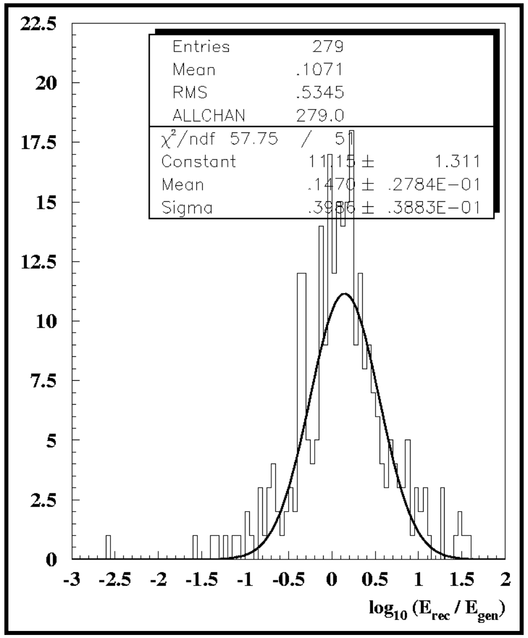

❖ Including effects of reconstruction and selection, PMT TTS, positioning, timing calibration accuracy and scattering.

❖ Below ~10 TeV angular error is dominated by ν-μ physical angle.

❖ Above ~10 TeV angular accuracy is better than 0.4° (reconstruction error).

❖ $\sigma_E / E \approx 3$ (1 TeV≤ E ≤10 TeV)

❖ $\sigma_E / E \approx 2$ (E >10 TeV)

❖ Below E ~ 100 GeV energy estimation via muon range measurement.

Background

Two kinds of physical background:

- **Muons produced by cosmic rays in the atmosphere (detector deep in the sea and selection of up-going events).**
- **Atmospheric neutrinos (cut in energy and angle for point sources).**

$$p \rightarrow \pi^{+}(+K^{+}\ldots) \rightarrow \mu^{+} + \nu_{\mu}$$

$$\rightarrow e^{+} + \overline{\nu}_{\mu} + \nu_{e}$$

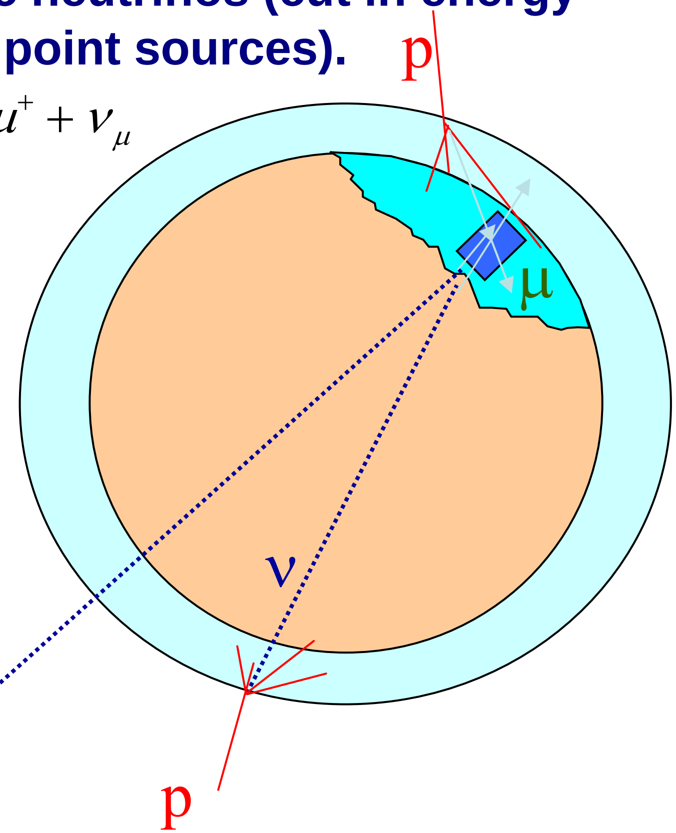

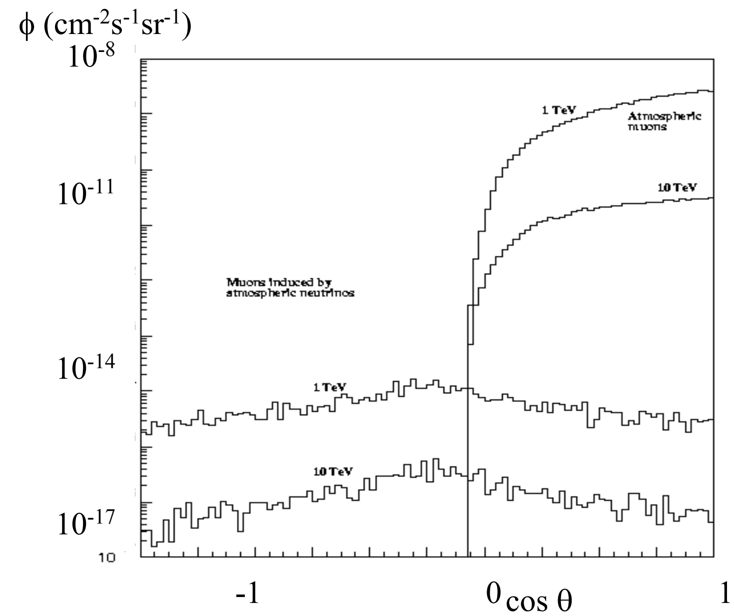

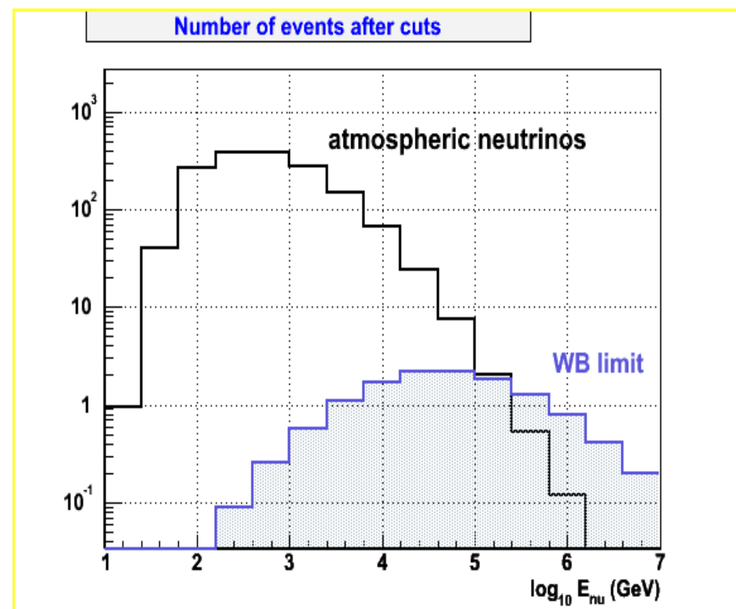

Muons seen by MACRO

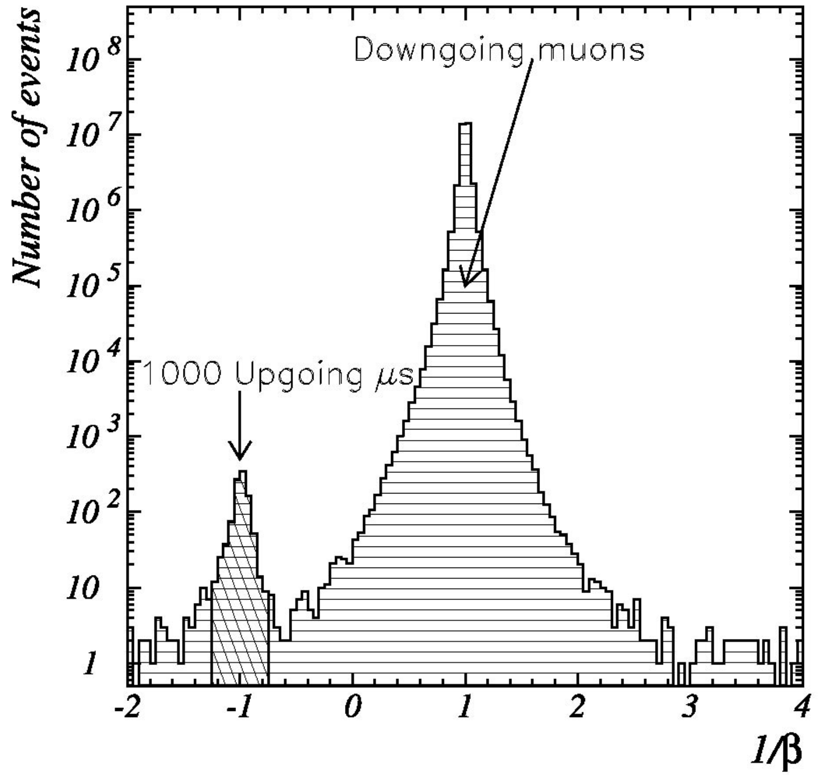

FIG. 2.—The $1/\beta$ distribution for the muon data sample collected with the full detector. The number of down-going muons is $\sim 33.8 \times 10^6$.

NEMO: Capo Passero

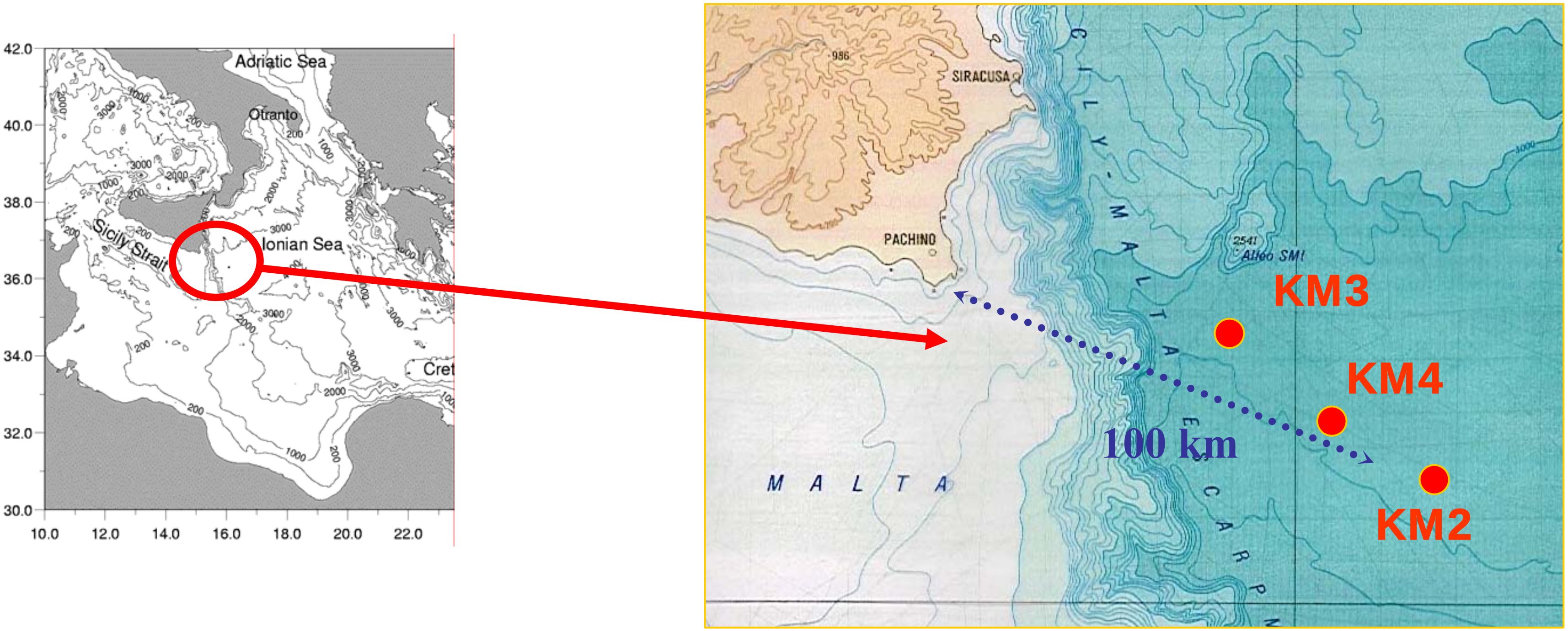

- KM2 36°10' N 16°19'E, depth 3350m (1: Jan '99)
- KM3 36°30' N 15°50'E, depth 3345m (1: Feb '99, 1: Aug'99, 2: Dec '99)
- KM4 36°19'N, 16°04'E, depth 3341m (2: Dec '99, 2: March '00, contiuing)

Coordinated Feasibility Study for a km3 detector

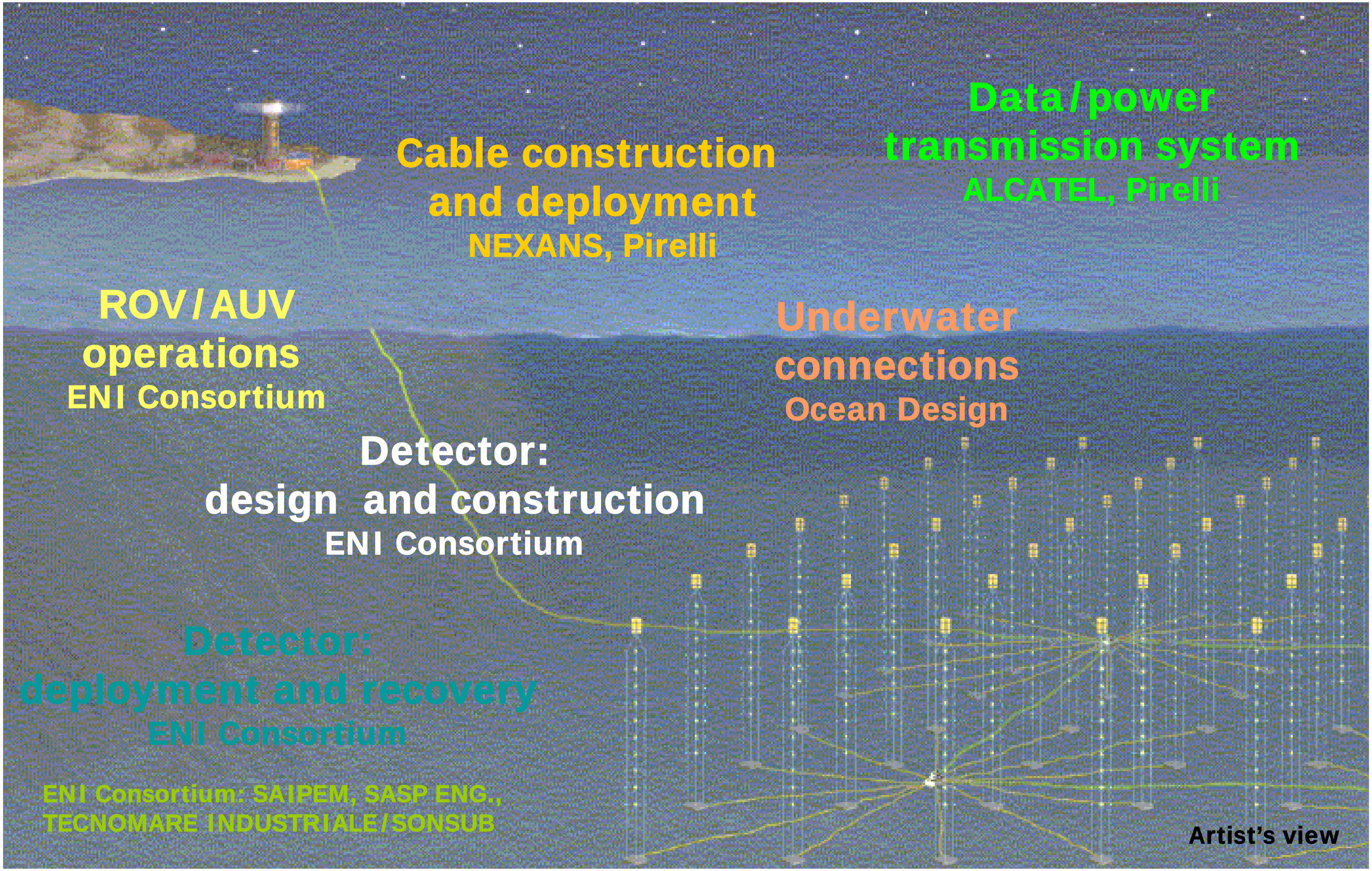

The telescope proposed by NEMO

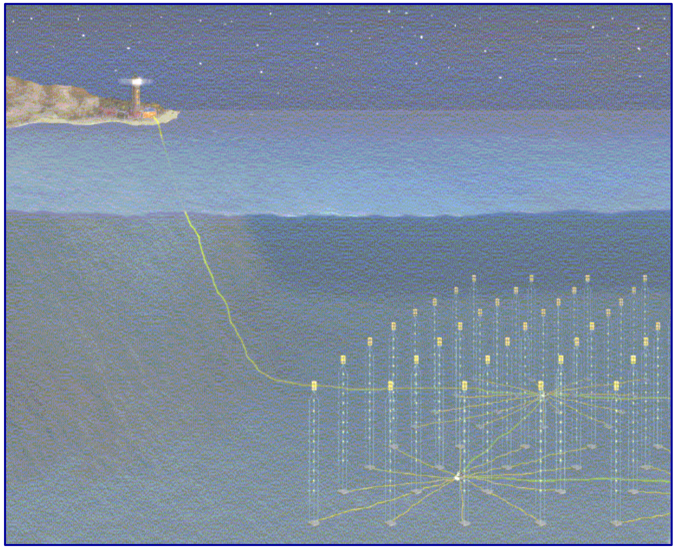

OPNEMO:

fast montecarlo code is designed to study the telescope performance as a function of:

- **detector geometry**
- **PMT dimensions, TTS**
- **water optical properties**

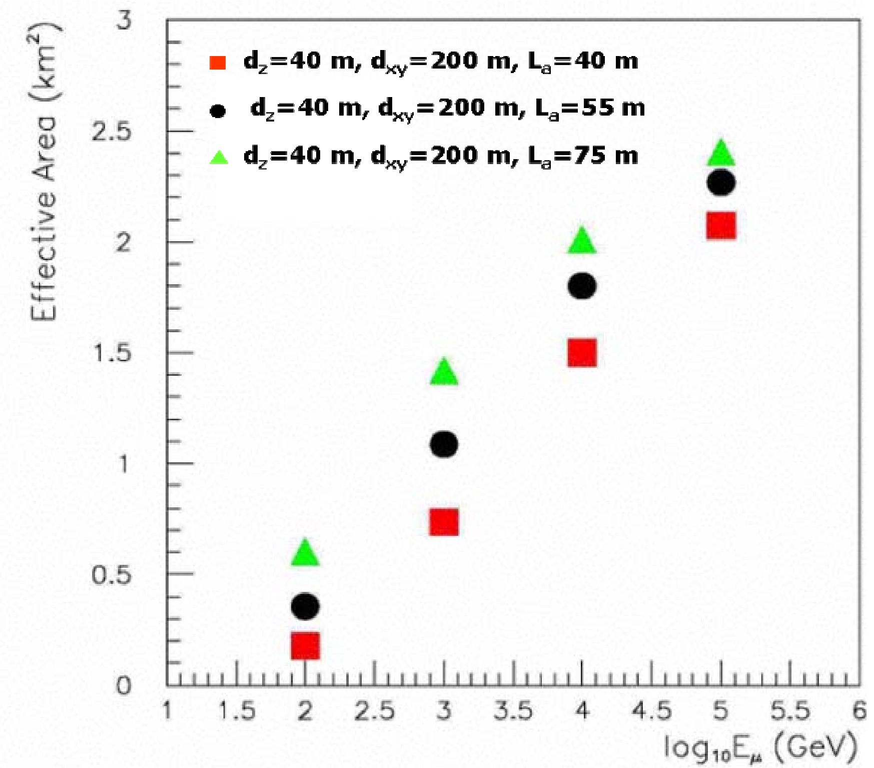

Simulations show that a detector of:

4096	**Optical Modules**
64	**Towers**
600m	**height**
200m	**distance between towers**
75m	**L_a (Capo Passero)**

May achieve:

>2km² trigger area

<0.3° angular resolution (median angle)

The NEMO tower

The tower designed by NEMO is a flexible structure tobe constructed in composite material:

fiberglass and dynema

tower height	750 m
distance between the lowest and the higest arm	600 m
number of arms	16
distance between the seabed and lowest arm	150 m
arm length	20 m
distance between arms	40 m
OM per arm (downward and upward directed)	4
OM per tower	64

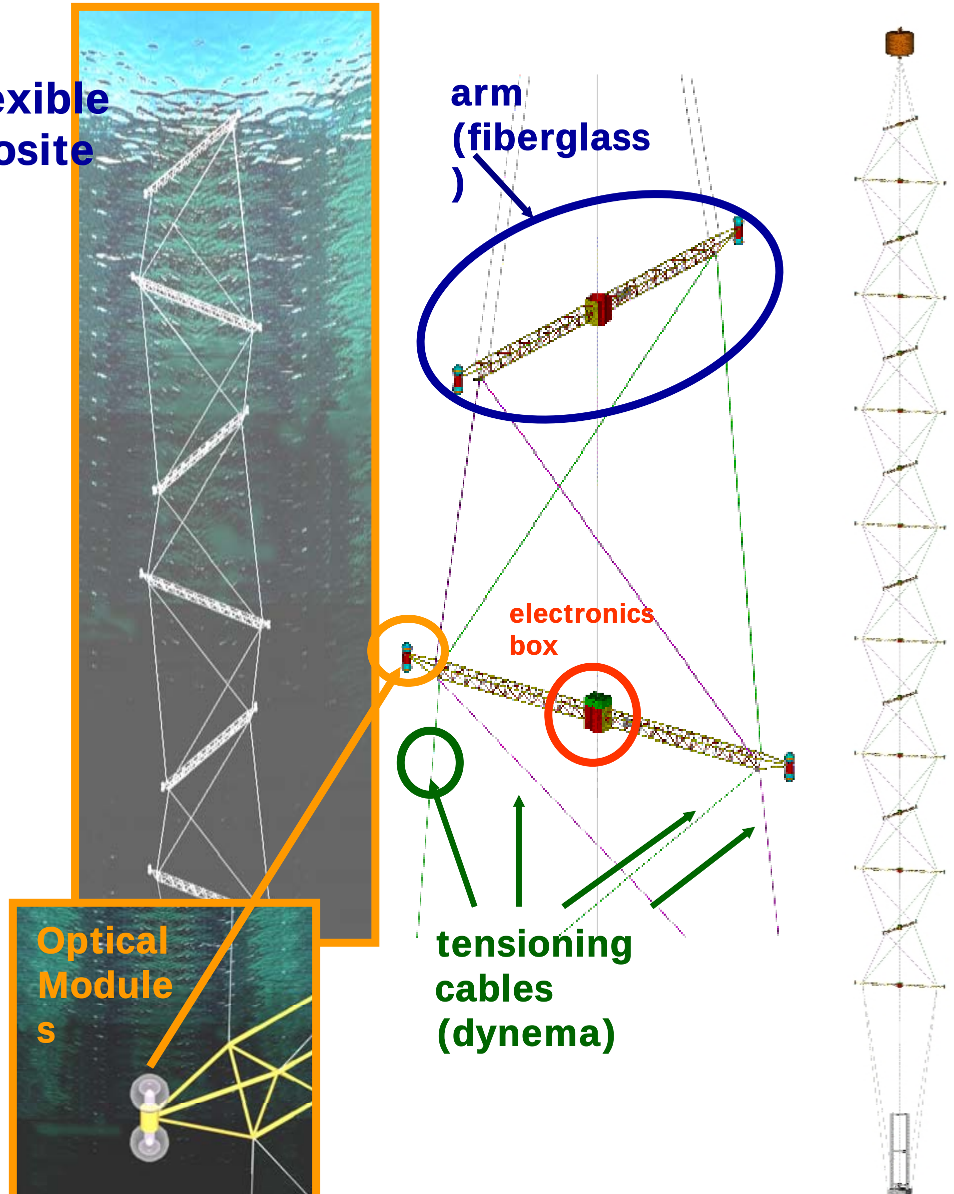

Deployment of the tower

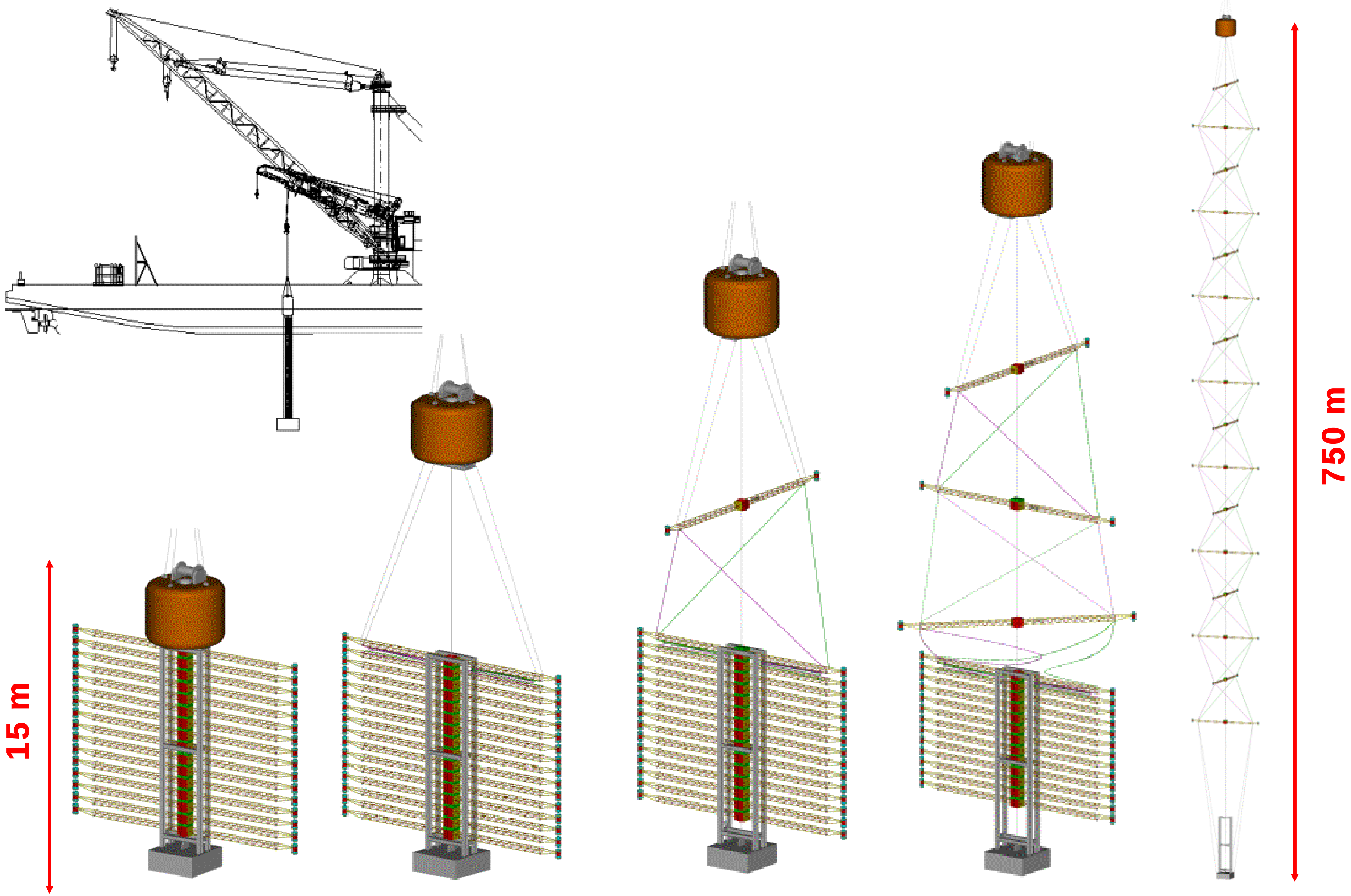

Cable Design

NEXANS in collaboration with INFN proposes the following solution:

- 100 km Electro-optical cable
- double armour
- 48 optical fibers
- 3 or 4 electrical conductors

AC solution

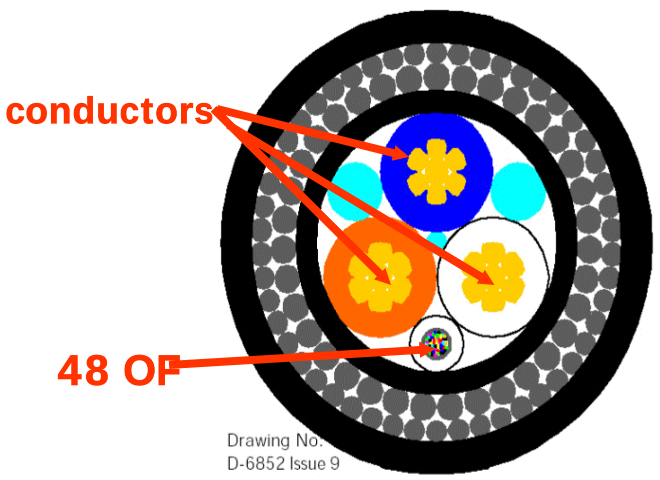

The use of 3 or 4 conductors is submitted to the use of:

- AC (three-phases)
- DC monopolar (sea return)
- DC bipolar (cable return)

DC solution (bipolar)

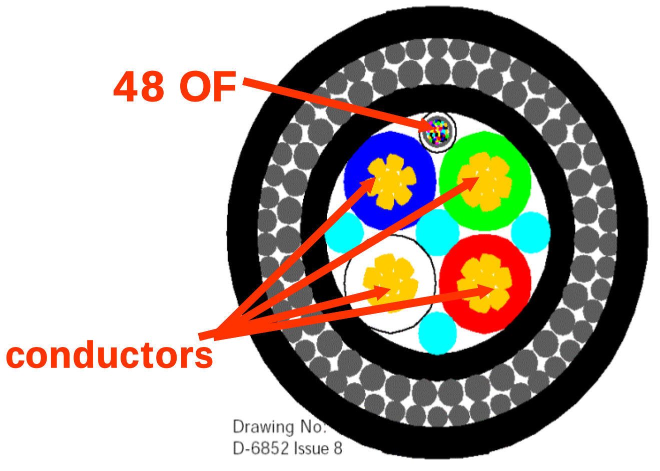

The NESTOR Neutrino Telescope Site

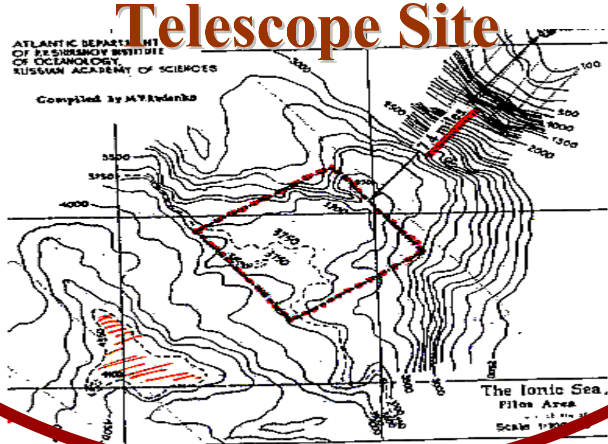

Site characteristics

- **a broad plateau:** 8x9 km² in area, 7.5 nautical miles from shore
- **depth:** ~4000m (→5200m)
- **transmission length:** 55 ± 10m at λ=460 nm
- **underwater currents:** <10 cm/s measured over the last 10 years
- **optical background:** ~50 kHz/OM due to K^{40} decay bioluminescence activity (1% of the experiment live time)
- **sedimentology tests:** flat clay surface on sea floor, good anchoring ground.

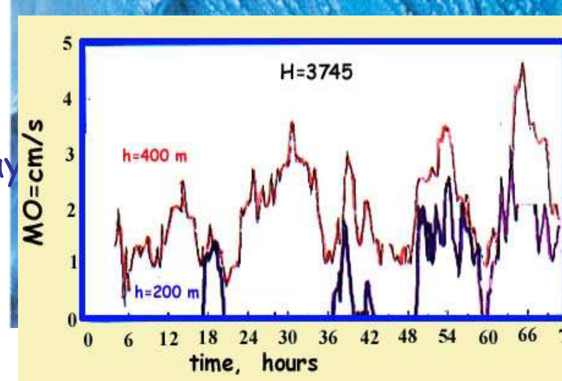

NESTOR DETECTOR

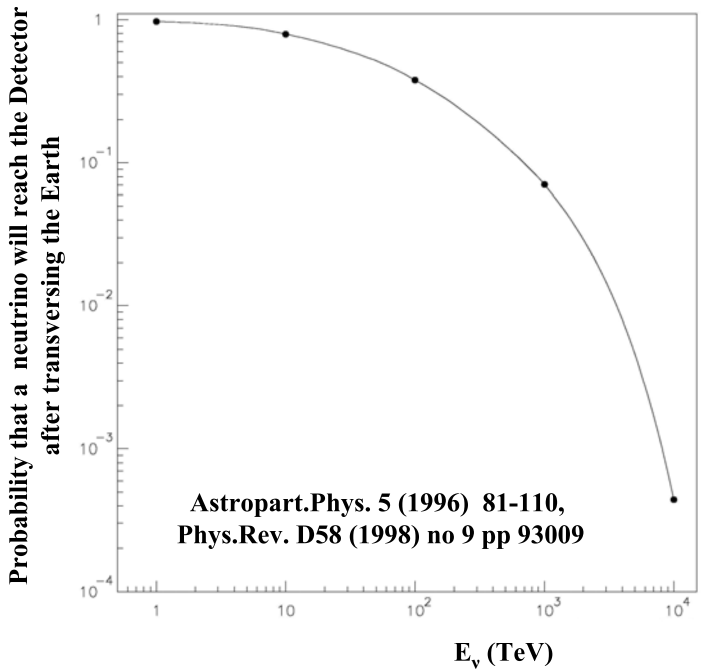

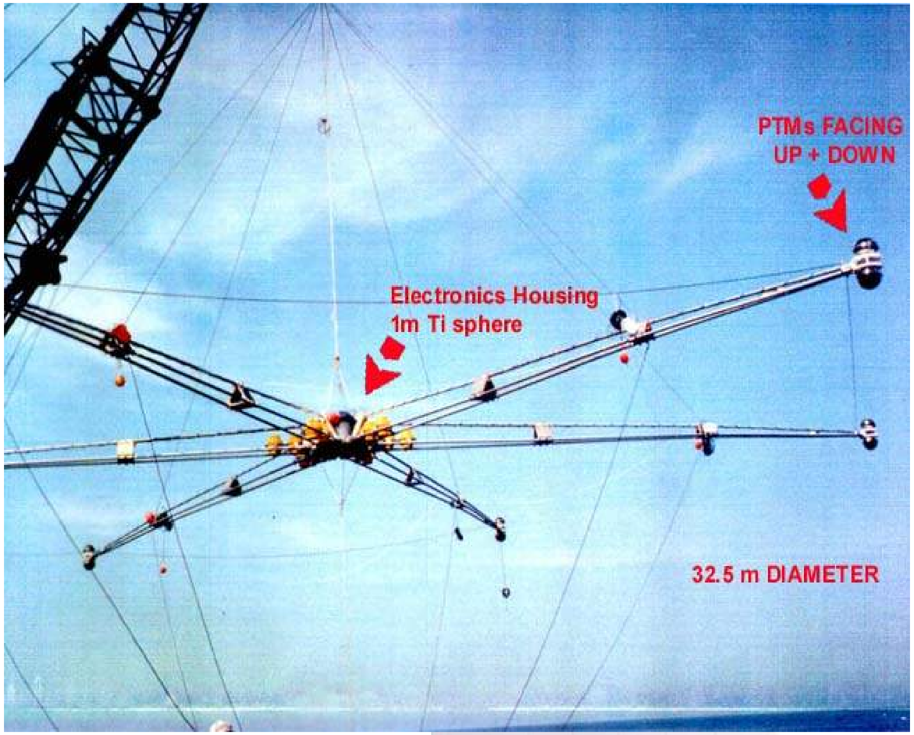

Energy threshold as low as 4 GeV

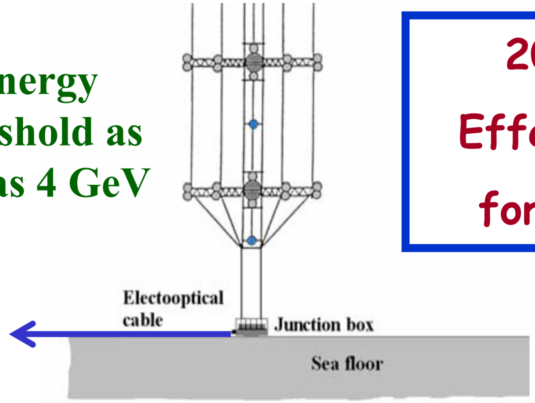

20 000 m^2
Effective Area
for E>10TeV

The future

Mediterranean Sites

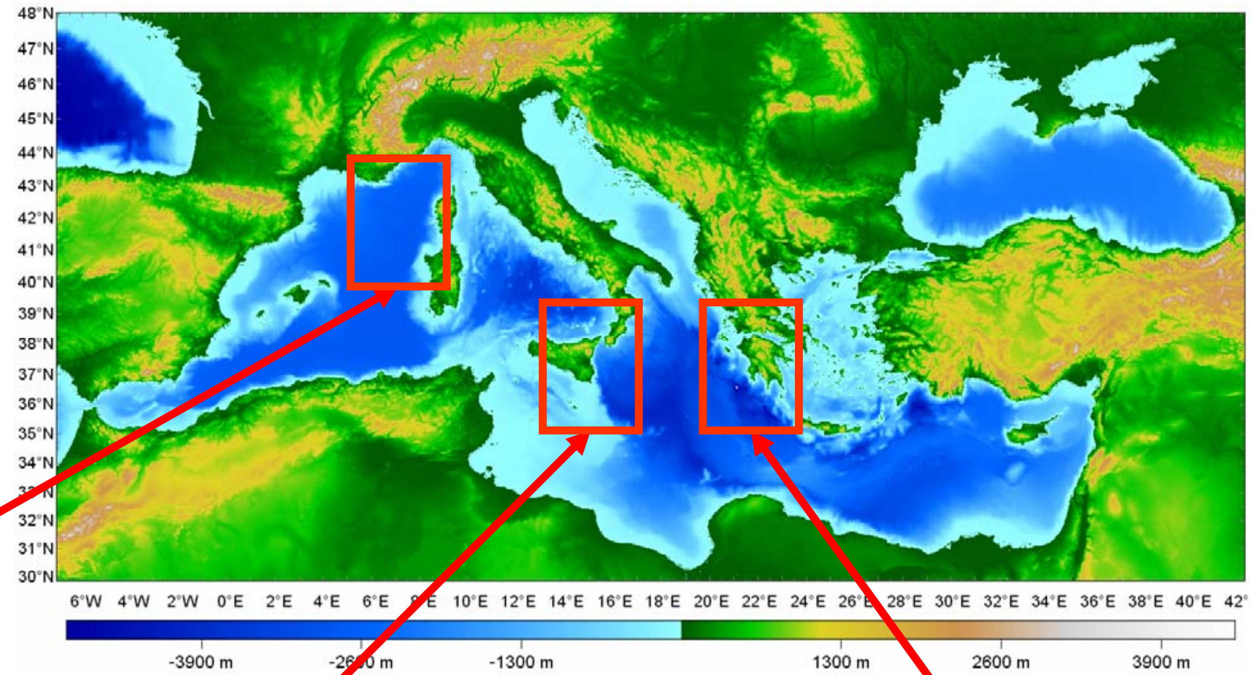

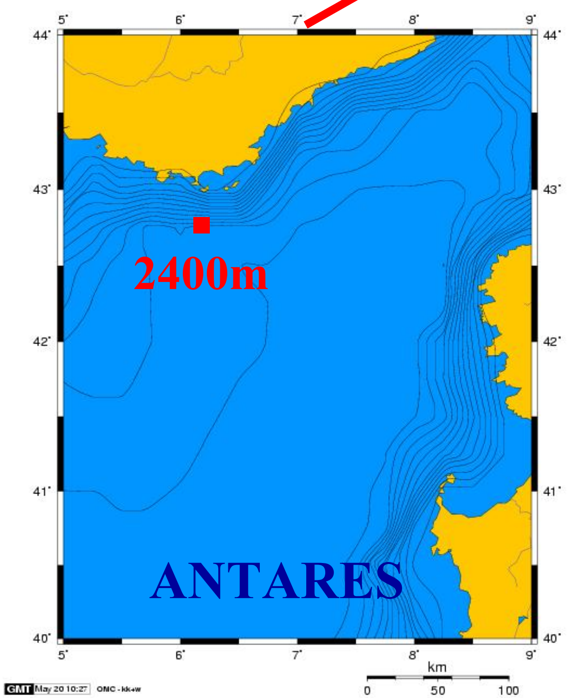

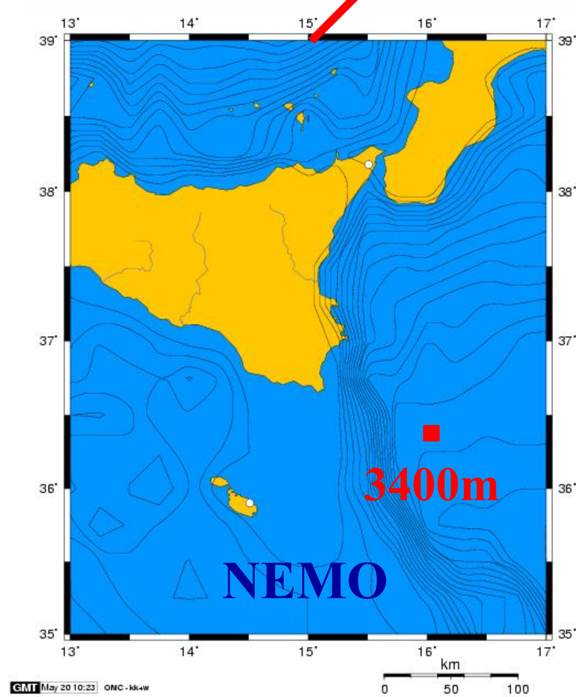

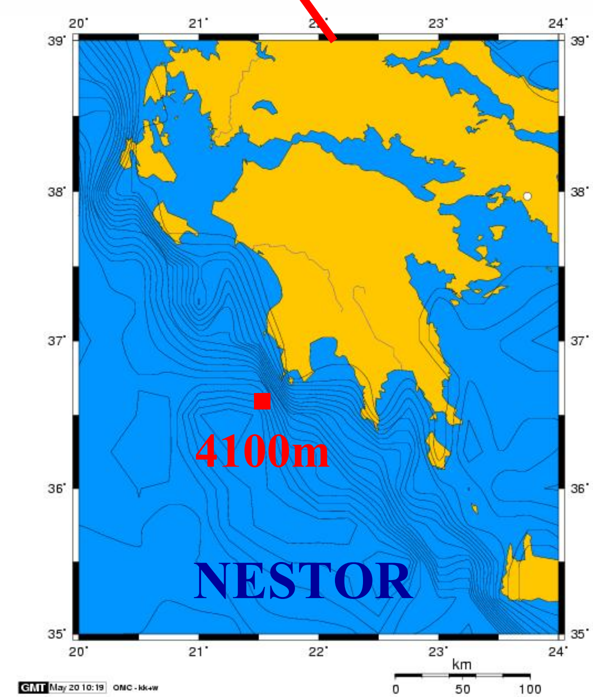

Km3Net

The KM3NeT Project

Design Study for a Deep Sea Facility in the Mediterranean for Neutrino Astronomy and Environmental Sciences

Physics Perspectives of KM3NeT
Status of Current Deep-Sea Projects

Objectives and Time Schedule for KM3NeT

Associated Sciences

Management and Status of Proposal

Institutions

- Institutes participating in the Design Study:

Cyprus: ***Univ. Cyprus***

France: ***CEA/Saclay, CNRS/IN2P3 Marseille, CNRS/IN2P3 Strasbourg, Univ. Haute Alsace***

Germany: ***Univ. Erlangen***

Greece: ***Hellenic Open Univ., NCSR "Demokritos", NOA/Nestor Inst., Univ. Athens, Univ. Crete, Univ. Patras***

Italy: ***INFN (Bari, Bologna, Catania, LNS Catania, LNF Frascati, Genova, Messina, Pisa, Roma-1)***

Netherlands: ***NIKHEF (Univ. Amsterdam, Free Univ., Univ. Utrecht, Univ. Nijmegen)***

Spain: ***IFIC (CSIC, Univ. Valencia), U.P. Valencia***

United Kingdom: ***Univ. Leeds, Univ. Sheffield, Univ. Liverpool***

Coordinator: Uli Katz, Erlangen

Requested Funding

- **Detailed evaluation of financial needs still ongoing**
- **Estimated overall budget of Design Study of the order 15 MEuro.**

Amount requested from EU:

10 MEuro over 3 years

KM3NeT Milestones

End 2004	**start design study**
Mid 2006	**conceptual design ready**
End 2007	**technical design ready**
2008-2012	**construction**
2009-…	**operation**

Associated Sciences

- *Great interest in long term deep-sea measurements in many different scientific communities:*
  - *Biology*
  - *Oceanography*
  - *Environmental sciences*
  - *Geology and geophysics*
  - *. . .*
- *Communication with ESONET established*
- *Plan: include the associated science communities in the design phase to understand and react to their needs*